[Supporting Information]

Hypercrosslinking chiral Brønsted acids into porous organic polymers for efficient heterogeneous asymmetric organosynthesis

Yuwei Zhang,[1,3] Zhenwei Zhang,[1] Si Ma,[1] Ji Jia,[1] Hong Xia,[2] and Xiaoming Liu,[*1]

[1]College of Chemistry, Jilin University, Changchun, 130012, P.R. China.

[2]State Key Laboratory on Integrated Optoelectronics, College of Electronic Science and Technology, Jilin University, Changchun 130012, P.R. China.

[3]Laboratory of Preparation and Applications of Environmental Friendly Materials (Jilin Normal University), Ministry of Education, Changchun, 130103, P.R. China

Email: xm_liu@jlu.edu.cn

Contents

Section 1. General Information

^{1}H spectra were recorded on a Avance III-400 NMR spectrometer, where chemical shifts (δ in ppm) were determined with a residual proton of the solvent as standard. Solid-state ^{13}C CP/MAS NMR measurement was recorded using a Bruker AVANCE III 400 WB spectrometer at a MAS rate of 5 kHz and a CP contact time of 2 ms. Elemental analyses were carried out on an Elementar model vario EL cube analyzer. The infrared spectra were recorded from 400 to 4000 cm-1on an Avatar FT-IR 360 spectrometer by using KBr pellets. UV/Vis spectra have been carried out on a Perkin Elmer Lambda 950 spectrophotometer within the wavelength range 200–700 nm. Field emission scanning electron microscopy was performed on a SU8020 model HITACHI microscope. Transmission electron microscopy was performed on a JEOL model JEM-2100 microscope. The sample was prepared by drop-casting a supersonic methanol suspension of polymer onto a copper grid. Powder X-ray diffraction data were recorded on a PANalytical BV Empyrean diffractometer by depositing powder on glasssubstrate, from 2θ = 1.5° to 40° with 0.02° increment at 25 °C. Thermogravimetric analysis (TGA) was performed on a TA Q500 thermogravimeter by measuring the weight loss while heating at a rate of 10 °C min^{-1} from room temperature to 800 °C under nitrogen. Nitrogen sorption isotherms were measured at 77 K with a JW-BK 132F analyzer. Before measurement, the samples were degassed in vacuum at 120 °C for more than 10 h. The Brunauer-Emmett-Teller (BET) method was utilized to calculate the specificsurface areas and pore volume. X-Ray photoelectron spectroscopy (XPS) was measured with an ESCALAB 250 spectrometer (Thermo Scientific, Waltham, MA) with monochromatic Al Kαradiation (1486.6 eV). The content of residual Fe (0.2~0.4 wt%) in obtained polymers was determined by Perkin-Elmer ICP-OES optima 3300DV spectroscopy. The enantiomeric excesses were determined by HPLC analysis using a *Waters Technologies* 1525 Series instrument (column: CHIRACEL OD-H, 0.46 cm ø, 25 cm). The catalytic products were quantified by GC analysis (Shimadzu GC-2014C) using an SE-30 column (30 m × 0.25 mm × 0.25 μm). The melting point was recorded on a melting point apparatus (MPA100, Stanford Research Systems, Inc.). GC-MS was performed using a QP2010 gas chromatography mass spectrometer (GC-2010 coupled with a GC-MS QP-2010, Shimadzu) equipped with a DB-5MS column (30 m × 0.25 mm × 0.25 μm, Agilent).

The column temperature was programmed from 50 °C (2 min hold) to 270 °C at 10 °C min^{-1}. Mass spectra were obtained by the electron-impact (EI) at 70 eV using the fullscan mode.

Section 2. Materials and Synthesis

The reactants used in the experiment were purchased from Energy Chemical unless otherwise stated. Deuterated solvents and n-Butyllithium solution in hexanes (1.6 M) were obtained from J&K Scientific. Formaldehyde dimethyl acetal (FDA), anhydrous $FeCl_3$ and 1,2-dichloroethane (DCE) were obtained from Aladdin. Other organic solvents for reactions were distilled over activated MS 4Å and used under nitrogen atmosphere.

Synthesis of (R)-2,2'-bis(methoxymethoxy)-1,1'-binaphthalene[1]

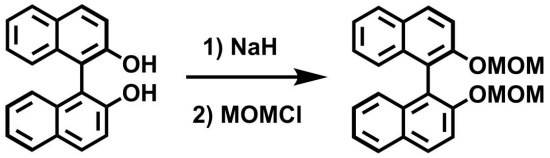

To a flame-dried flask fitted with a stir-bar and addition funnel was added NaH (60% dispersion in mineral oil, 1.3 g, 54.2 mmol, 3.0 equiv) and THF (30 mL). The reaction was cooled to 0 °C. R-(+)-BINOL (5.0 g, 17.5mmol, 1.0 equiv) was then added as one portion. The reaction mixture was stirred at 0 °C for 1 h. MOMCl (2.9 mL, 38.3 mmol, 2.2 equiv) was then added dropwise. The reaction was allowed to stir at 0 °C for 10 min. After completion, the reaction mixture was quenched with saturated aq. NH_4Cl, extracted with Et_2O, and washed with brine. The organic layer was dried with $MgSO_4$ and the solvent was removed via rotary evaporation. The crude product mixture was purified via column chromatography (EtOAc/hexane: 1/40), white foam (5.7 g, 92% yield). ^{1}H NMR (400 MHz, $CDCl_3$) δ: 7.99 (d, *J* = 8.0 Hz, 2H, Ar*H*), 7.91 (d, *J* = 8.0 Hz, 2H, Ar*H*), 7.61 (d, *J* = 8.0 Hz, 2H, Ar*H*), 7.39-7.35 (m, 2H, Ar*H*), 7.27-7.23 (m, 2H, Ar*H*), 7.19-7.17(d, *J* = 8.0 Hz, 2H, Ar*H*), 5.12-5.01 (m, 4H, -OC*H*$_2$OCH$_3$), 3.17 (s, 6H, -OCH$_2$OC*H*$_3$) ppm.

Synthesis of (R)-3,3'-diiodo-2,2'-bis(methoxymethoxy)-1,1'-binaphthalene[2]

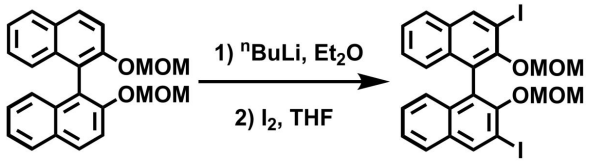

To a flame-dried flask equipped with a stir bar was added MOM-protected binapthyl (3.0 g, 8.0 mmol 1.0 equiv), and then Et_2O (30 mL). 1.6 M ^nBuLi (15 mL, 20 mmol, 2.5 equiv) was added to the reaction. The reaction mixture was allowed to stir for 4 hours at room temperature. The reaction mixture was then cooled to -78 °C and I_2 (3.02 g, 35.4 mmol, 2.5 equiv) was added as one portion. The reaction was allowed to slowly warm to room temperature and stir overnight. After completion, the reaction mixture was quenched with saturated aq. NH_4Cl, extracted with Et_2O, and washed with 10% aq. $Na_2S_2O_3$ followed by brine solution. The organic layer was dried with $MgSO_4$ and the solvent was removed via rotary evaporation. The crude product mixture was then purified via column chromatography with eluent (EtOAc/hexane: 1/40) on silica gel. Light yellow powder. (5.2 g, 70% yield). ^1H NMR (400 MHz, $CDCl_3$) δ: 8.75 (s, 2H, Ar*H*), 7.81 (d, *J* = 8.0Hz, 2H, Ar*H*), 7.47-7.43 (m, 2H, Ar*H*), 7.34-7.31 (m, 2H, Ar*H*), 7.21 (d, *J* = 8.0Hz, 2H, Ar*H*), 4.48, 4.72 (m, 4H, -OC*H*$_2$OCH$_3$), 2.62 (s, 6H, -OCH$_2$OC*H*$_3$) ppm.

Synthesis of (R)-3,3'-diaryl-2,2'-bis(methoxymethoxy)-1,1'-binaphthalene[3]

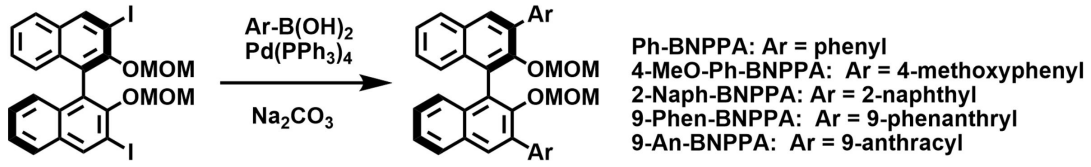

(R)-3,3'-diiodo-2,2'-bis(methoxymethoxy)-1,1'-binaphthalene (1.0 equiv) and $Pd(PPh_3)_4$ (10 mol%) were mixed in DME (40 mL) in a round bottom flask at room temperature under an argon atmosphere. To the mixture with stirring were added phenylboronic acid (3.5 equiv) and 2 M aqueous Na_2CO_3 solution (5.2 equiv). The resulting mixture was stirred and heated to reflux for 10 h, cooled to room temperature, and passed through a pad of Celite. The organic solution was evaporated to give a residue. The residue was dissolved in CH_2Cl_2, washed with

saturated aqueous NH_4Cl, water, brine, dried over Na_2SO_4, and concentrated to give a crude product. Purification was carried by column chromatography (EtOAc/hexane: 1/10) to give product.

(R)-3,3'-diiodo-2,2'-bis(methoxymethoxy)-1,1'-binaphthalene. White foamy product, yield: 85%. ^{1}H NMR (400 MHz, $CDCl_3$) δ: 7.95 (s, 2H, Ar*H*), 7.90 (d, *J* = 8.0 Hz, 2H, Ar*H*), 7.77 (d, *J* = 8.0Hz, 2H, Ar*H*), 7.49-7.29 (m, 12H, Ar*H*), 4.41-4.36 (m, 4H, -OC*H*$_2$OCH$_3$), 2.34(s, 6H, -OCH$_2$OC*H*$_3$) ppm.

(R)-3,3'-Bis(4-methoxyphenyl)-2,2'-Bis(methoxymethoxy)-1,1'-binaphthyl. Light yellow powder, yield: 87%. ^{1}H NMR (400 MHz, $CDCl_3$) δ: 7.94 (s, 2H, Ar*H*), 7.91 (d, *J* =8.0Hz, 2H, Ar*H*), 7.74-7.71 (m, 4H Ar*H*), 7.45-7.41 (m, 4H Ar*H*), 7.04-6.80 (m, 6H, Ar*H*), 4.45-4.39 (m, 4H, -OC*H*$_2$OCH$_3$), 3.90 (s, 6H, ArOC*H*$_3$), 2.36 (s, 6H, -OCH$_2$OC*H*$_3$) ppm.

(R)-3,3'-Bis(2-naphthyl)-2,2'-Bis(methoxymethoxy)-1,1'-binaphthyl. White foamy product, yield: 91%.^{1}H NMR (400 MHz, $CDCl_3$) δ: 8.26 (s, 2H, Ar*H*), 8.10 (s, 2H, Ar*H*), 8.0-7.92 (m, 10H Ar*H*), 7.56-7.33 (m, 10H Ar*H*), 4.48-4.45 (m, 4H, -OC*H*$_2$OCH$_3$), 2.36 (s, *6*H, -OCH$_2$O OC*H*$_3$) ppm.

(R)-3,3'-Bis(9-phenanthryl)-2,2'-Bis(methoxymethoxy)-1,1'-binaphthyl. White powder, yield, 90 %. ^{1}H NMR (400 MHz, $CDCl_3$) δ: 8.83-8.76 (m, 4H, Ar*H*), 8.13-7.84 (m, 10H Ar*H*), 7.73-7.34 (m, 10H Ar*H*), 4.62-4.30 (m, 4H, -OC*H*$_2$OCH$_3$), 2.18-2.13 (d, 6H, OC*H*$_3$) ppm.

(R)-3,3'-Bis(9-anthryl)-2,2'-Bis(methoxymethoxy)-1,1'-binaphthyl. White powder, yield, 91 %. ^{1}H NMR (400 MHz, $CDCl_3$) δ: 8.56 (s, 2H, Ar*H*), 8.11-7.92 (m, 8H， Ar*H*), 7.94 (d, *J* = 8.0 Hz, 2H Ar*H*), 7.82 (d, *J* = 8.0 Hz, 2H Ar*H*), 7.67 (d, *J* = 8Hz, 2H Ar*H*), 7.54-7.40 (m, 10H, Ar*H*), 7.25-7.22 (t, *J* = 12.0Hz, 2H, Ar*H*), 4.30-4.23 (m, 4H, -OC*H*$_2$OCH$_3$), 1.89 (s, *6*H, -OCH$_2$OC*H*$_3$) ppm.

Synthesis of (*R*)-3,3'-diaryl-2,2'-dihydroxy-1,1'-dinaphthyl[3b]

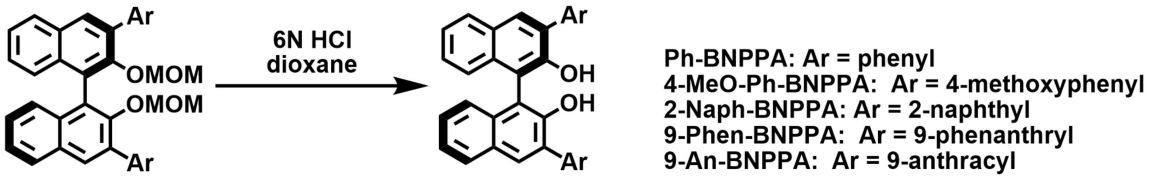

6N HCl (10.0 mL) was added to a solution of MOM protected binol (1.1 mmol) in dioxane (15 mL). The resulting solution was heated to 60 °C for 12 h. The reaction mixture was cooled to room temperature and quenched by addition of sat. $NaHCO_3$ solution. The product was extracted into CH_2Cl_2 and washed with water, then brine. The combined organics were dried over Na_2SO_4, filtered and concentrated to yield the crude product as a pink solid. Trituration/washing with CH_2Cl_2:Et_2O (1:10) provided pure product.

(*R*)-3,3'-diphenyl-2,2'-dihydroxy-1,1'-dinaphthyl. White powder, yield, 90%. ^{1}H NMR (400 MHz, $CDCl_3$) δ: 8.05 (s, 2H, Ar*H*), 7.96 (d, *J* = 8.0 Hz, 2H, Ar*H*), 7.77 (d, *J* = 4.0 Hz, 4H, Ar*H*), 7.54 (t, *J* = 12.0 Hz, 4H, Ar*H*), 7.46-7.41 (m, 4H, Ar*H*), 7.37-7.33 (m, 4H, Ar*H*), 7.29-7.27 (m, 2H, Ar*H*), 5.38 (s, 2H, Ar-O*H*) ppm.

(*R*)-3,3'-bis(4-methoxyphenyl)-2,2'-dihydroxy-1,1'-binaphthyl. White powder (yield, 95). ^{1}H NMR (400 MHz, $CDCl_3$) δ: 8.24(s, 2H, Ar*H*), 8.17(s, 2H, Ar*H*), 8.0-7.90(m, 10H, Ar*H*), 7.56-7.31(m, 10H, Ar*H*), 5.50(s, 2H, Ar-O*H*), 3.90(s, 6H, ArOC*H*$_3$) ppm.

(*R*)-3,3'-bis(2-naphthyl)-2,2'-dihydroxy-1,1'-binaphthyl. Light yellow powder, yield: 95%. ^{1}H NMR (400 MHz, $CDCl_3$) δ: (s, 2H, Ar*H*), 8.16 (s, 2H, Ar*H*), 8.0-7.90 (m, 10H, Ar*H*), 7.56-7.31 (m, 10H, Ar*H*), 5.38 (s, 2H, Ar-O*H*) ppm.

(R)-3,3'-bis(9-phenanthryl)-2,2'-dihydroxy-1,1'-binaphthyl. Light yellow powder, yield: 94%. ^{1}H NMR (400 MHz, $CDCl_3$) δ: 8.85-8.76 (m, 4H, Ar*H*), 8.12-8.10 (m, 10H, Ar*H*), 8.00-7.88 (m, 7H, Ar*H*), 8.71-7.44 (m, 15H, Ar*H*), 5.34 (s, 2H, Ar-O*H*) ppm.

(R)-3,3'-bis(9-anthryl)-2,2'-dihydroxy-1,1'-binaphthyl. Light yellow powder, yield: 93%. ^{1}H NMR (400 MHz, $CDCl_3$) δ: 8.60(s, 2H, Ar*H*), 8.13-7.88(m, 12H, Ar*H*), 7.70-7.43(m, 14H, Ar*H*) 5.08(s, 2H, Ar-O*H*) ppm.

Synthesis of (R)-3,3'-Diaryl-1,1'-binaphthyl phosphate[4]

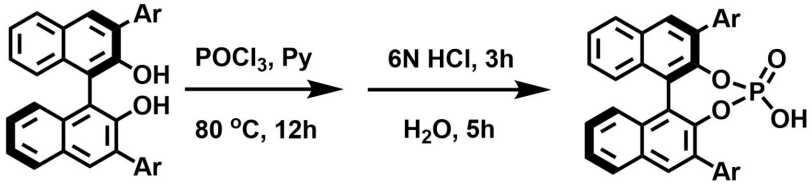

Ph-BNPPA: Ar = phenyl
4-MeO-Ph-BNPPA: Ar = 4-methoxyphenyl
2-Naph-BNPPA: Ar = 2-naphthyl
9-Phen-BNPPA: Ar = 9-phenanthryl
9-An-BNPPA: Ar = 9-anthracyl

(R)-3,3'-diphenyl-[1,1'-binaphthalene]-2,2'-diol (833 mg, 1.90 mmol, 1.0 equiv.) was suspended in anhydrous pyridine (7.0 mL). To the mixture was added freshly distilled $POCl_3$ (355 μL, 3.80 mmol, 2.0 equiv.) in one portion, which maintain a gentle reflux. After 12 h of additional stirring at ambient temperature, the reaction mixture was pull into water 50 mL. The combined organic layers were dried over anhydrous Na_2SO_4, filtered and concentrated in vacuo. The resultant crude phosphoroyl chloride (light yellow foamy solid), then it was refluxed in 6N HCl (10 mL) for 3 h. Absolute CH_2Cl_2 (15 mL) was then shaken with the mixture, and the layers were separated. The aqueous layer was extracted with CH_2Cl_2 (3×20 mL), then dried over anhydrous Na_2SO_4, filtered and liberated of solvents under reduced pressure.

(R)-3,3'-Dipheny-1,1'-binaphthyl phosphate (Ph-BNPPA). White powder, yield: 92%. ^{1}H NMR (400 MHz, $CDCl_3$) δ: 7.95-7.91 (m, 6H, Ar*H*), 7.73(d, *J* = 8 Hz, 4H, Ar*H*), 7.47-7.38 (m, 4H, Ar*H*), 7.25-7.18 (m, 4H, Ar*H*), 7.09-7.04 (m, 2H, Ar*H*) ppm. ^{13}C NMR (100 MHz, $CDCl_3$) δ: 146.07, 145.97, 143.74, 141.74, 141.30, 137.82, 134.37, 132.28, 130.89, 130.06, 128.30, 128.03, 127.09, 126.99, 126.20, 125.87, 125.39, 132.12 ppm.

(R)-3,3'-Bis(4-methoxyphenyl)-1,1'-binaphthyl phosphate (4-MeOph-BNPPA). Light yellow powder, yield: 82%. ^{1}H NMR (400 MHz, $CDCl_3$) δ: 7.95 (s, 4H, Ar*H*), 7.55-7.47 (m, 6H, Ar*H*), 7.38-7.27 (m, 6H, Ar*H*), 6.77 (d, *J* = 8Hz, 4H, Ar*H*), 3.56 (s, 4H, ArOC*H*$_3$) ppm. ^{13}C NMR (100 MHz, $CDCl_3$) δ: 158.93, 145.24, 145.15, 133.85, 133.82, 131.88, 131.47, 131.06, 130.80, 129.50, 128.29, 127.04, 126.16, 125.69, 122.71, 113.59, 55.02 ppm.

(R)-3,3'-Bis(2-naphthyl)-1,1'-binaphthyl phosphate (2-Naph-BNPPA). Light yellow powder, yield: 91%.^{1}H NMR (400 MHz, $CDCl_3$) δ: 8.24-7.93 (m, 10H, Ar*H*), 7.80-7.31 (m, 12H, Ar*H*), 7.18 (m, 2H, Ar*H*) ppm. ^{13}C NMR (100 MHz, $CDCl_3$) δ: 146.88, 146.79, 144.47, 139.88, 136.11, 134.43, 133.23, 132.28, 131.13, 130.94, 128.41, 128.36, 127.45, 127.27, 127.04, 126.20, 125.77, 125.24, 124.54, 123.58 ppm.

(R)-3,3'-Bis(9-phenanthryl)-1,1'-binaphthyl phosphate (9-Phen-BNPPA). Light yellow powder, yield: 83%.^{1}H NMR (400 MHz, DMSO) δ: 8.91 (m, 4H, Ar*H*), 8.31-8.02 (m, 8H, Ar*H*), 7.73-7.55 (m, 16H, Ar*H*) ppm. ^{13}C NMR (100 MHz, $CDCl_3$) δ: 146.37, 146.26, 134.07, 133.10, 132.74, 132.50, 131.58, 131.55, 131.38, 130.31, 130.10, 129.73, 129.40, 129.19, 127.73, 127.66, 127.53, 127.46, 127.16, 126.83, 126.54, 123.69, 123.32, 122.26 ppm.

(R)-3,3'-Bis(9-anthryl)-1,1'-binaphthyl phosphate (9-An-BNPPA). Light yellow powder, yield: 85%).^{1}H NMR (400 MHz, $CDCl_3$) δ: 8.30-7.96 (m, 10H, Ar*H*), 7.83-7.32 (m, 14H, Ar*H*), 7.11 (m, 4H, Ar*H*) ppm. ^{13}C NMR (100 MHz, $CDCl_3$) δ: 133.24, 133.04, 132.68, 131.16, 131.04, 130.80, 130.28, 128.41, 128.22, 127.45, 127.27, 126.61, 125.92, 125.49, 125.05, 124.76, 122.98 ppm.

Synthesis of BNPPA-HCPs

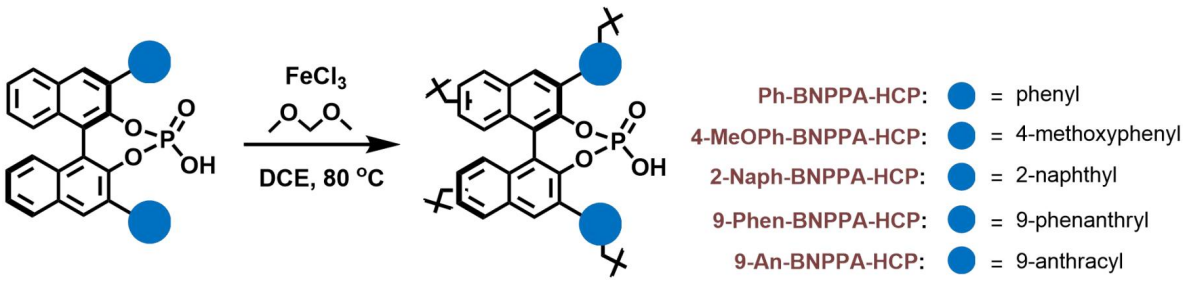

Ph-BNPPA-HCP. To the mixture of Ph-BNPPA (60 mg, 0.12 mmol) and FDA (40 µL, 0.5 mmol, 4 equiv.) in 2 mL 1,2-dichloroethane, dry $FeCl_3$ (74 mg, 0.5 mmol, 4 equiv.) was added at room temperature. The mixture was heated to 80 °C and stirred for 24 h under a nitrogen atmosphere. After cooling down to room temperature, the precipitated polymer network was filtered and washed with methanol, distilled water, dichloromethane and acetone successively, until the filtrate was nearly colorless. The further purification of the network was carried out by Soxhlet extraction from

methanol for 12 h. The product was dried in vacuum for 24 h at 60 °C to give dark brown powder (56.1 mg, 90.1%).

4-MeOph-BNPPA-HCP. 4-MeOph-BNPPA (50 mg, 0.083 mmol), FDA (29.5 µL, 0.33 mmol, 4eq), dry $FeCl_3$ (54.1 mg, 0.6 mmol, 4eq), and 2 mL of 1,2-dichloroethane were used in this polymerization (42.3 mg, 89.5%).

2-Naph-BNPPA-HCP. 2-Naph-BNPPA (50.0 mg, 0.09 mmol), FDA (32.0 µL, 0.36 mmol, 4eq), dry $FeCl_3$ (58.0 mg, 0.36 mmol, 4eq), and 2 mL of 1,2-dichloroethane were used in this polymerization (46.2 mg, 84%).

9-Phen-BNPPA-HCP. 9-Phen-BNPPA (50.0 mg, 0.071 mmol), FDA (25.5 µL, 0.28 mmol, 4eq), dry $FeCl_3$ (46.5 mg, 0.36 mmol, 4eq), and 2 mL of 1,2-dichloroethane were used in this polymerization (49.8 mg, 92%).

9-An-BNPPA-HCP. 9-An-BNPPA (50.0 mg, 0.071 mmol), FDA (25.5 µL, 0.28 mmol, 4eq), dry $FeCl_3$ (46.5 mg, 0.36 mmol, 4eq), and 2 mL 1,2-dichloroethane were used in this polymerization (49.7 mg, 92%).

General Procedure for the Enantioselective Transfer Hydrogenation by Chiral Brønsted Acid-based Hypercrosslinked Polymers

A centrifuge vial was charged with 3-Phenyl-2*H*-1,4-benzoxazin (10.5 mg, 0.19 mmol), Hantzsch dihydropyridine (15.8 mg, 0.24 µmol, 1.25 eq.) and the catalyst (5 mol%). $CHCl_3$ (1.5 mL) was added and the mixture was stirred for 4 h at room temperature. In case of a homogeneous reaction the solvent was removed in vacuum. In case of a heterogeneous reaction the catalyst was separated by centrifugation. The remaining solid catalyst was washed with $CHCl_3$ and again separated by centrifugation. The organic layers were combined and the solvents were removed in vacuum. The conversion was determined by ^{1}H-NMR analysis of the crude product. The yield was determined after column chromatography (SiO_2, hexane/AcOEt = 40:1).

Section 3. Characterization of BNPPA-HCPs

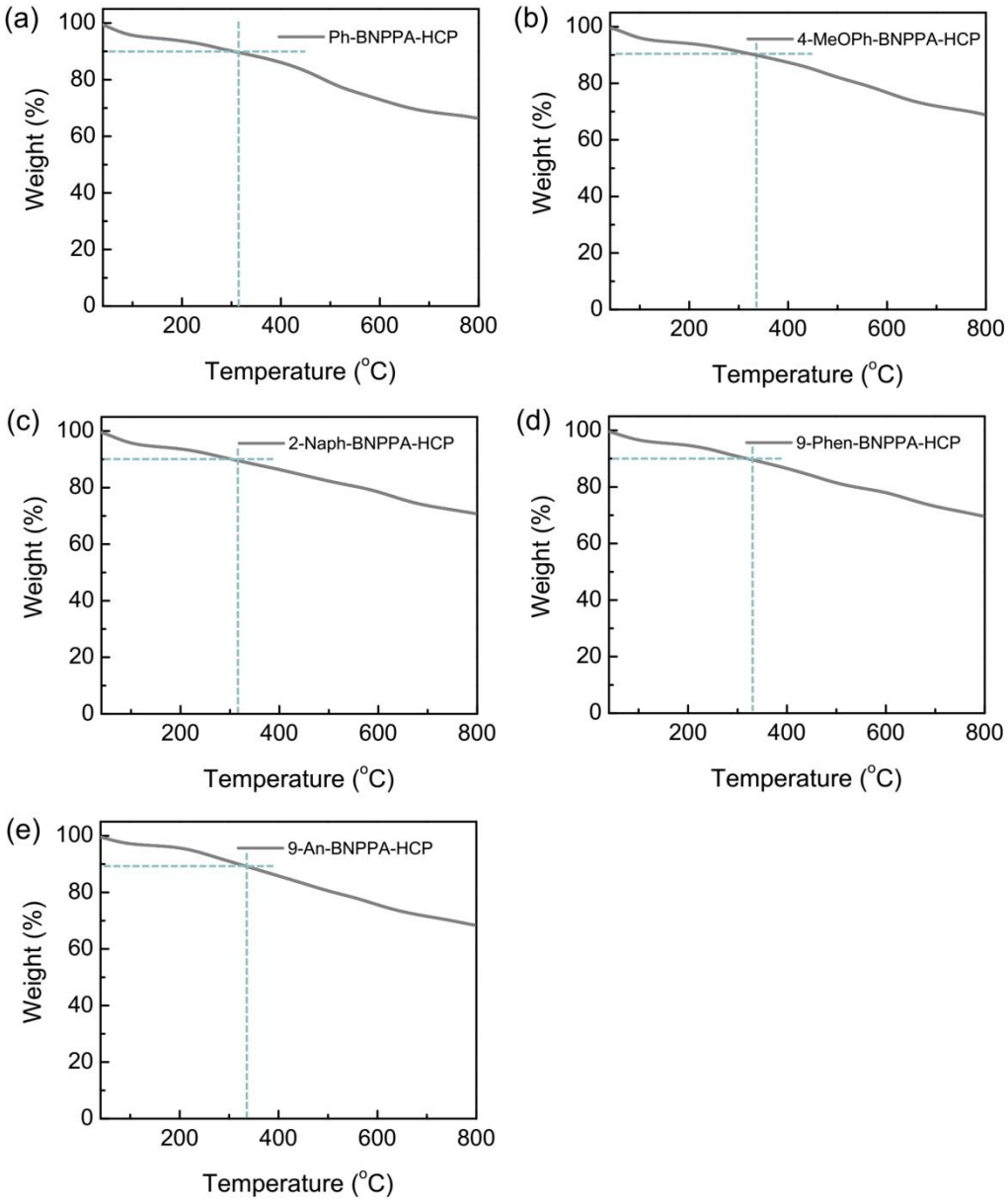

Figure S1. TGA curves of BNPPA-HCPs under nitrogen atmosphere. The TGA patterns suggested that all polymers are thermally stable, that indicated by retaining more than 90% of their weight up to 300 °C. The weight loss for BNPPA-HCPs at low temperature may be due to the adsorbed matters in the pores.

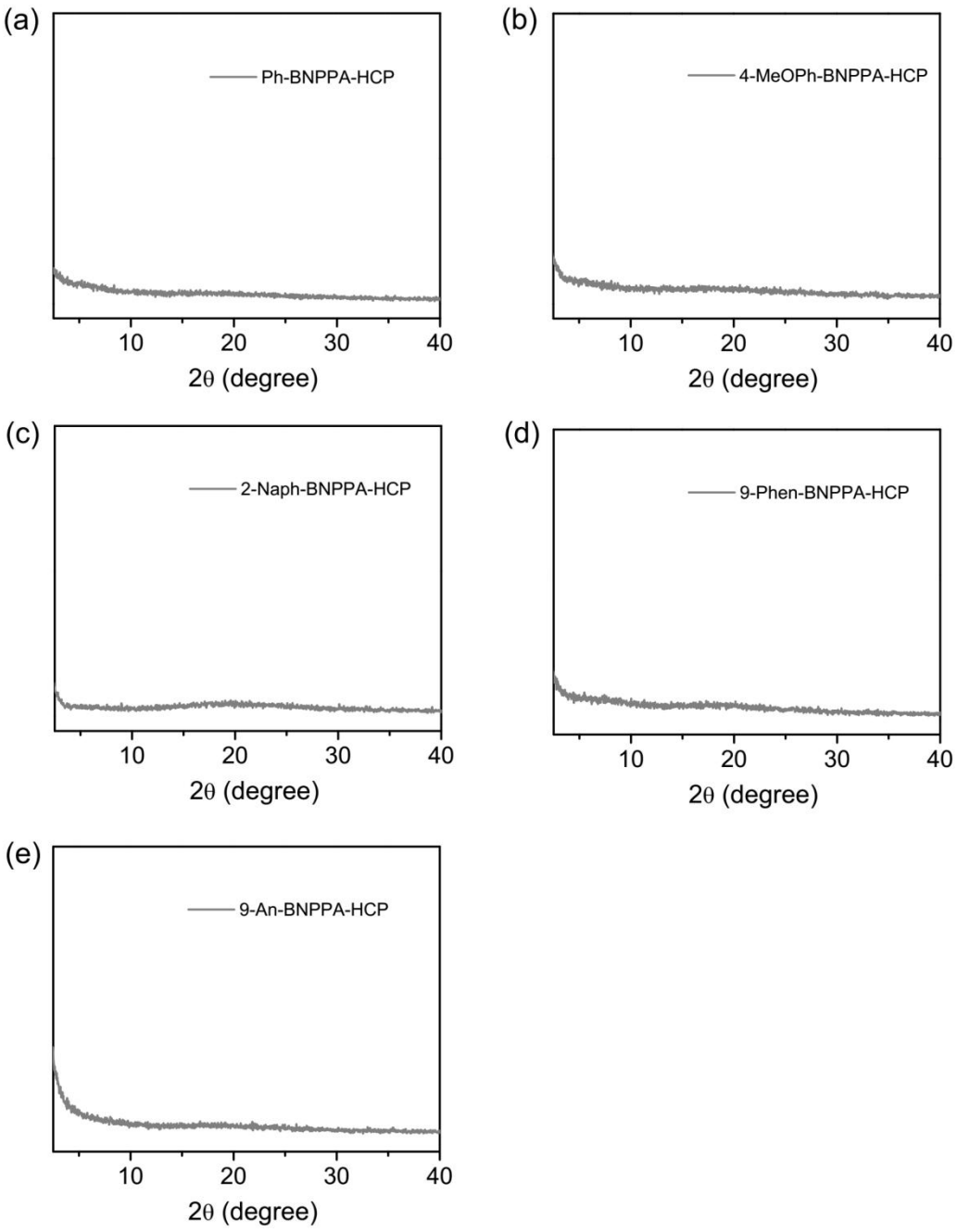

Figure S2. PXRD curves of BNPPA-HCPs. The PXRD patterns do not give any strong diffraction peaks, indicating that all polymers are amorphous materials.

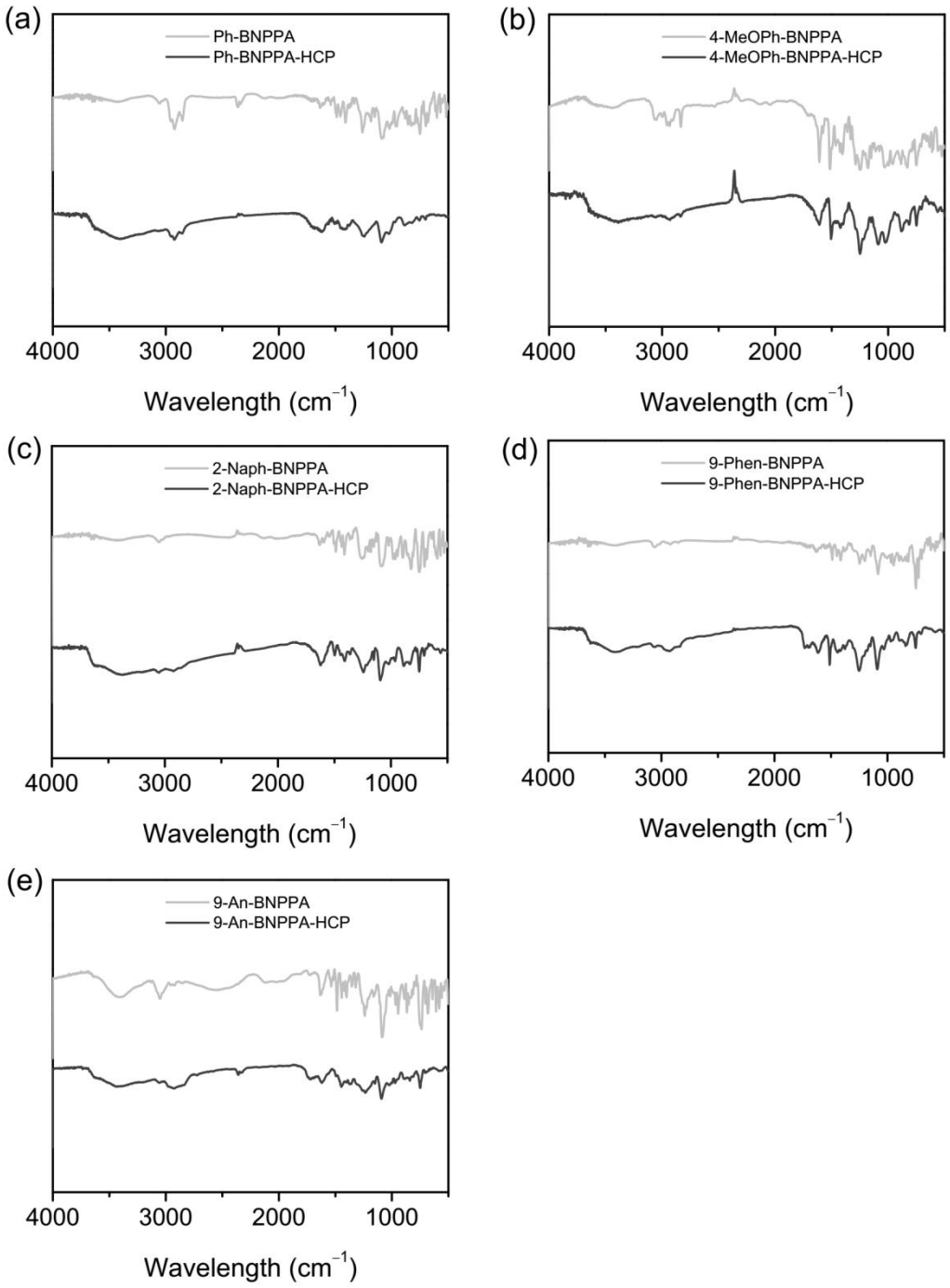

Figure S3. FT-IR spectra of BNPPA-HCPs and corresponding monomers. From FT-IR spectra, we found that the polymer also retains some characteristic peaks of the corresponding monomer. In addition, the weak peaks at ~2920 cm^{-1} could be attributed to C–H stretching vibration, which could originate from the structure of –CH_2– in the polymer network.

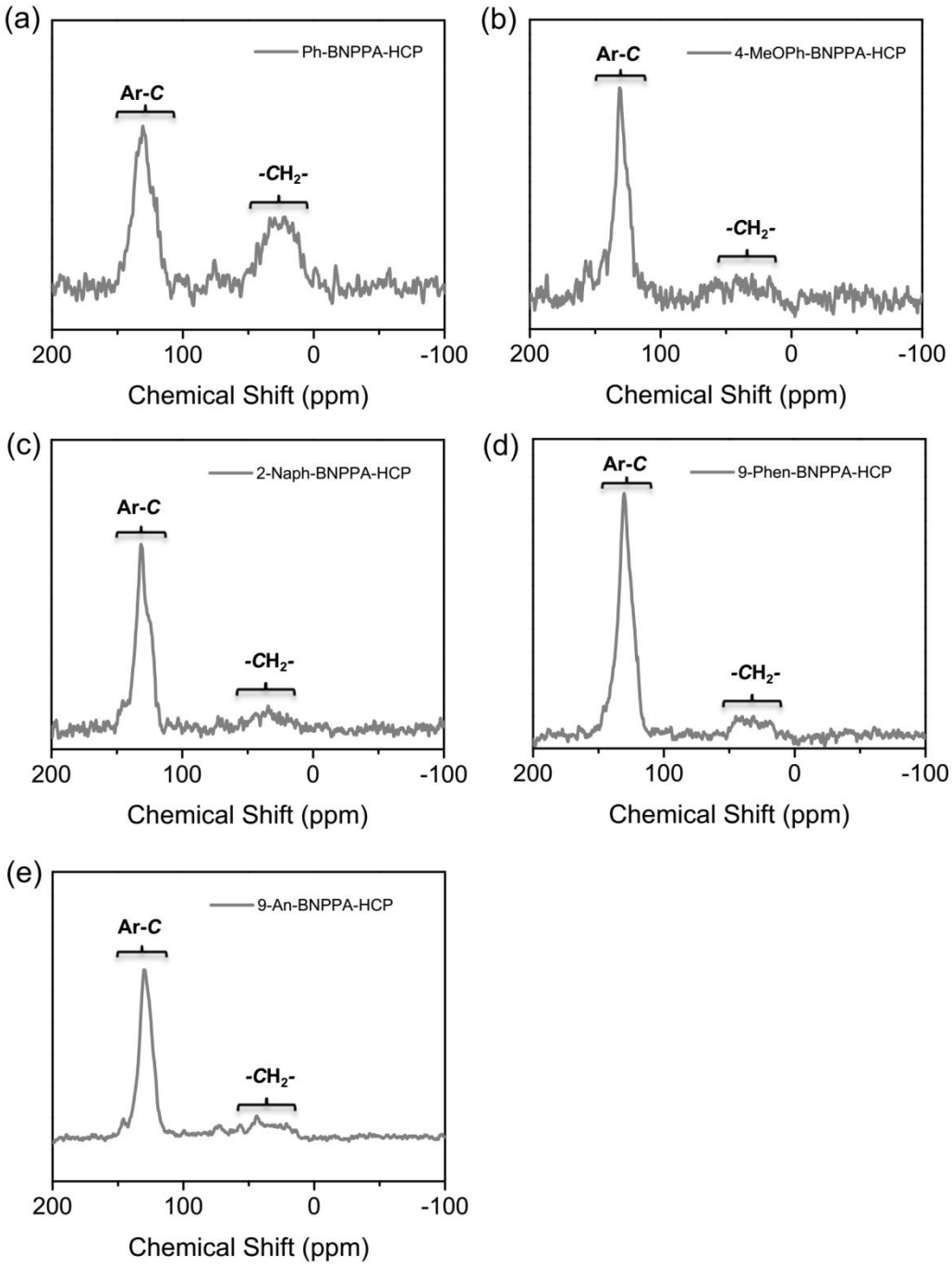

Figure S4. Solid-state ^{13}C CP-MAS NMR spectra of BNPPA-HCPs. The resonance peaks at 30~40 ppm can be assigned to the carbon in the methylene linker formed from the Friedel-Crafts reaction. The characteristic signals from 110 to140 ppm are assignable to substituted and nonsubstituted aromatic carbon in the polymer backbone.

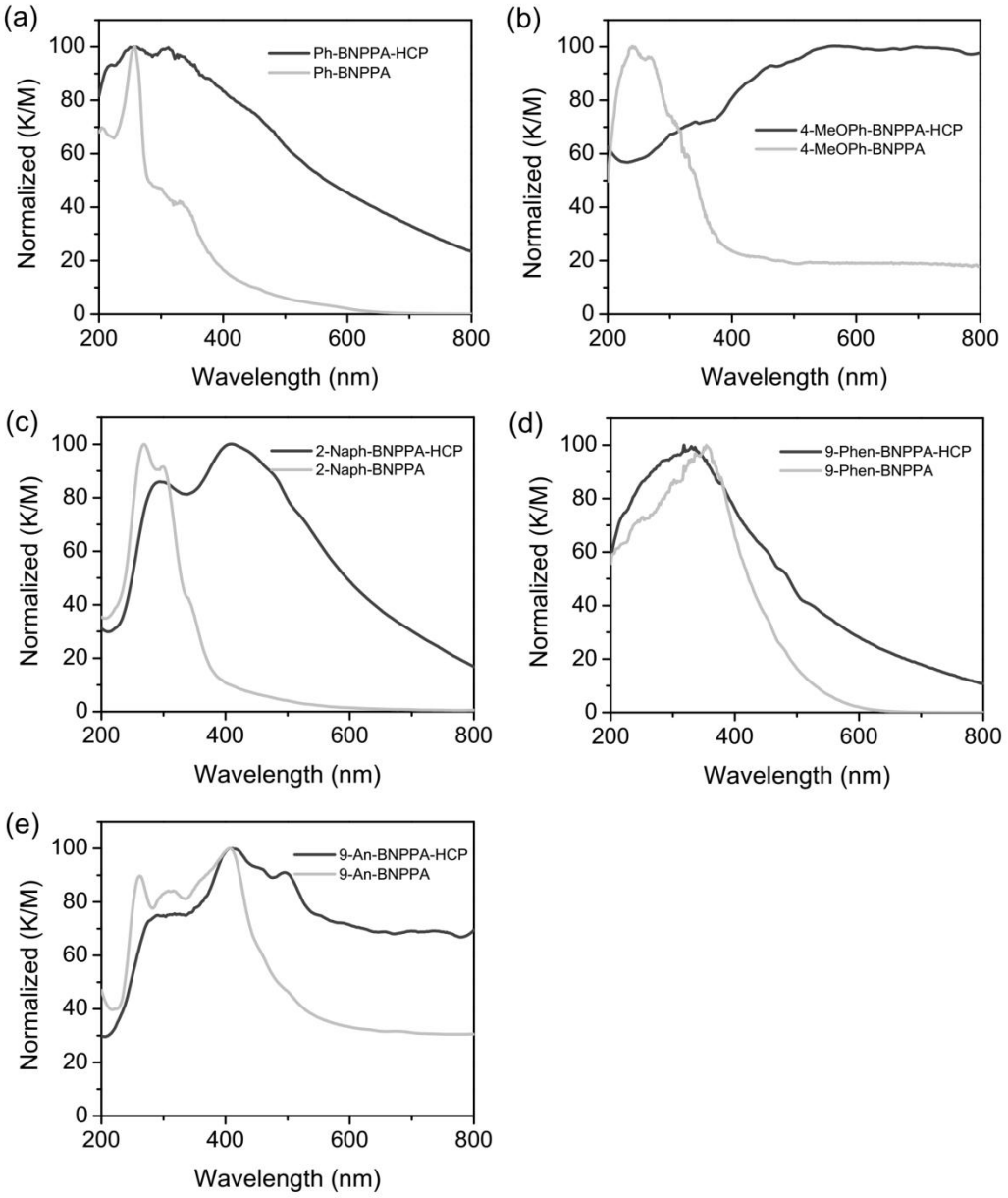

Figure S5. UV-vis DR spectra of BNPPAs and corresponding polymers BNPPA-HCPs.

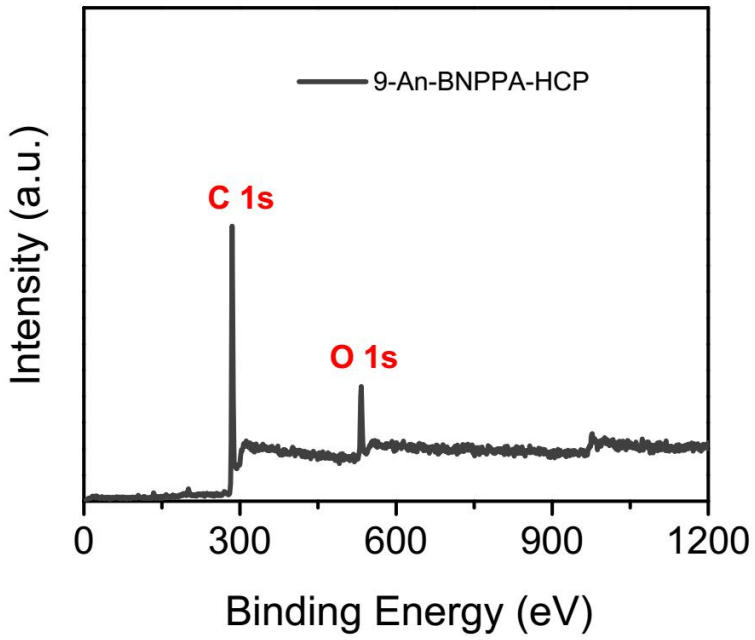

Figure S6. XPS pattern of 9-An-BNPPA-HCP recorded from 0 to 1200 eV.

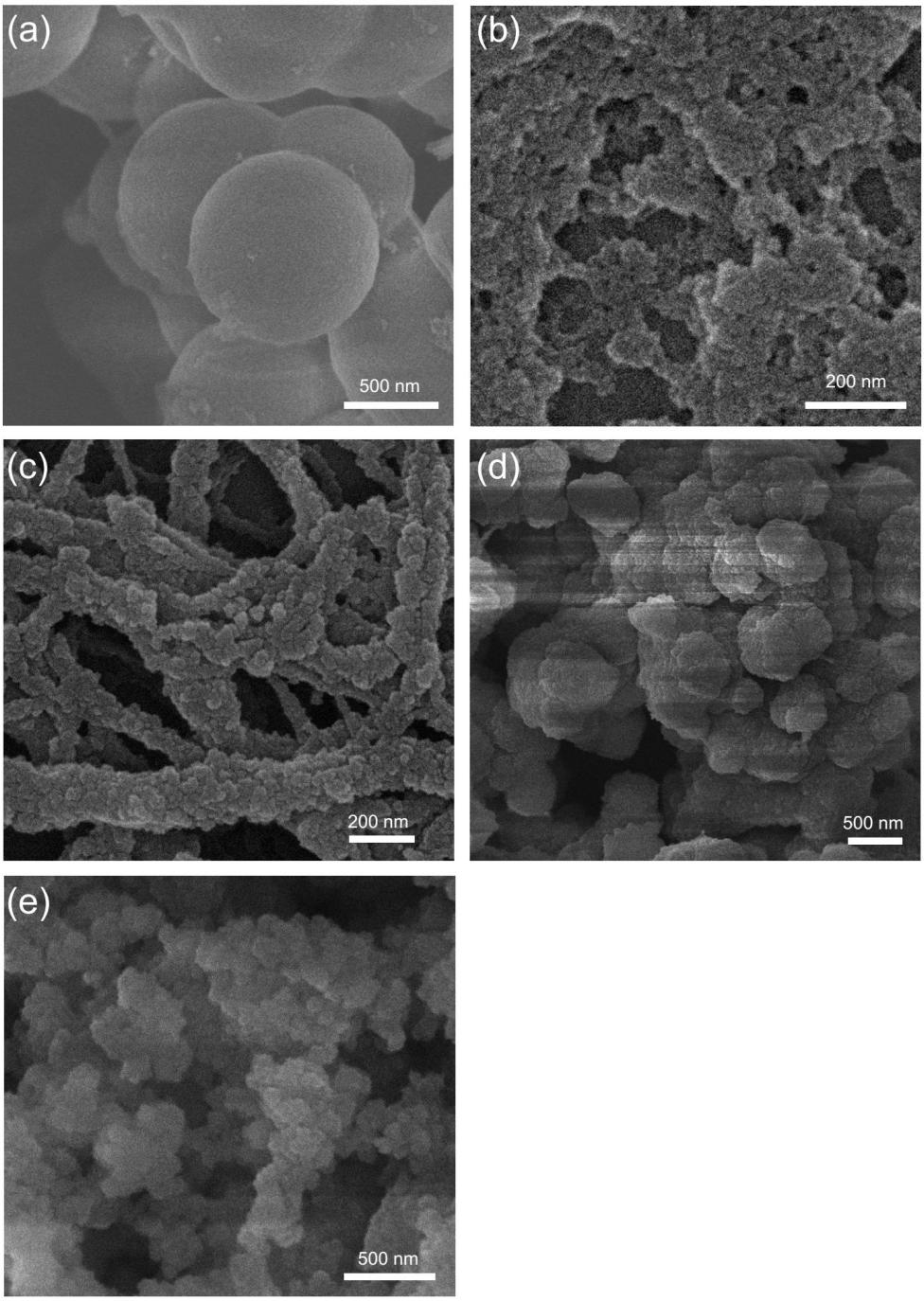

Figure S7. FE-SEM images of BNPPA-HCPs: (a) Ph-BNPPA-HCP (b) 4-MeOPh-BNPPA-HCP (c) 2-Naph-BNPPA-HCP (d) 9-Phen-BNPPA-HCP (e) 9-An-BNPPA-HCP.

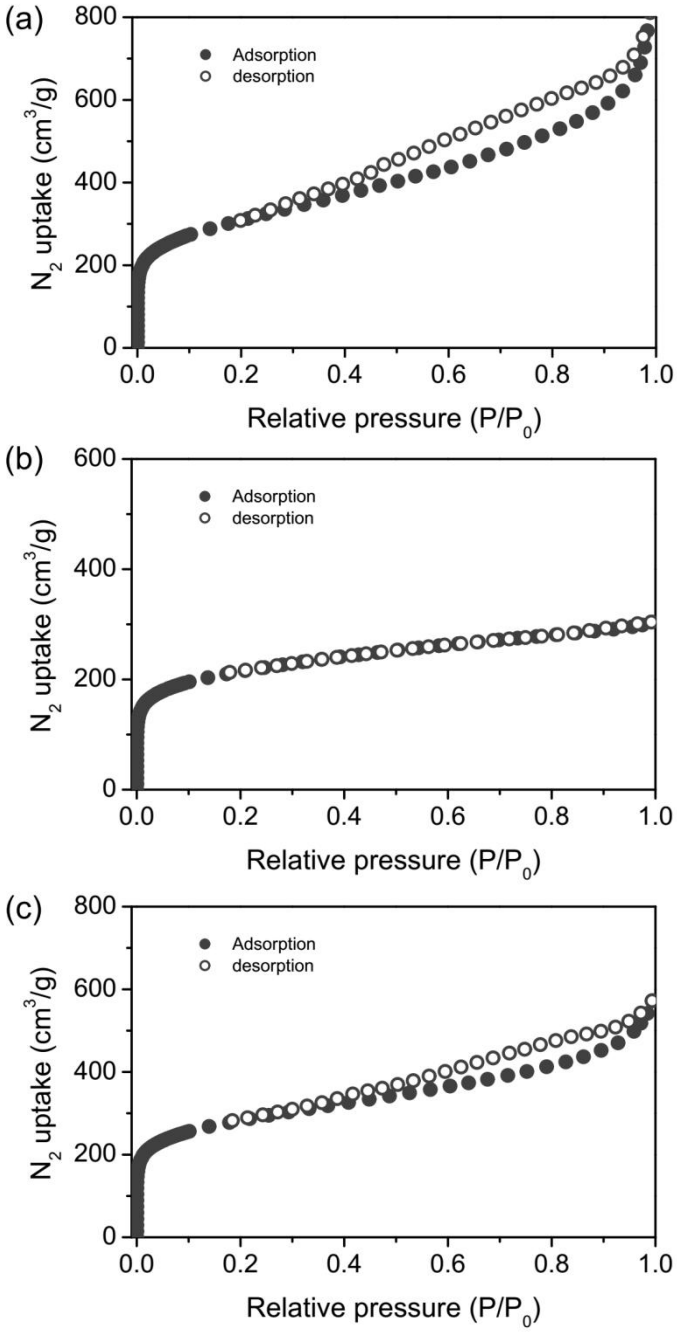

Figure S8. Nitrogen sorption isotherms of BNPPA-HCPs at 77 K: (a) Ph-BNPPA-HCP (b) 4-MeOPh-BNPPA-HCP (c) 9-Phen-BNPPA-HCP.

Section 4. Catalytic Data

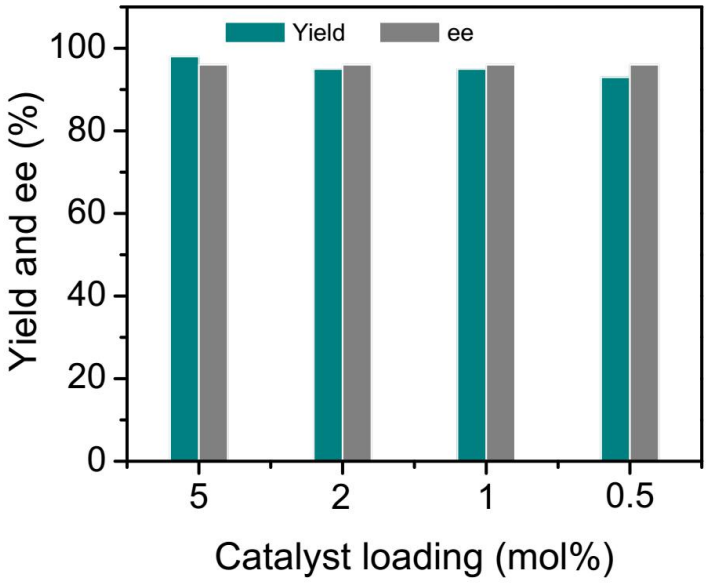

Figure S9. The effect of An-BNPPA-HCP loading on the reaction performances. Specific reaction process: 3-Phenyl-2H-1,4-benzoxazin (0.19 mmol), Hantzsch dihydropyridine (0.24 mmol), $CHCl_3$ (1.5 mL) and the catalyst (5 mol%, 2 mol%, 1 mol%, and 0.5 mol%) was added in 4 centrifuge vials and the mixture was stirred for 4h respectively at 25 °C.

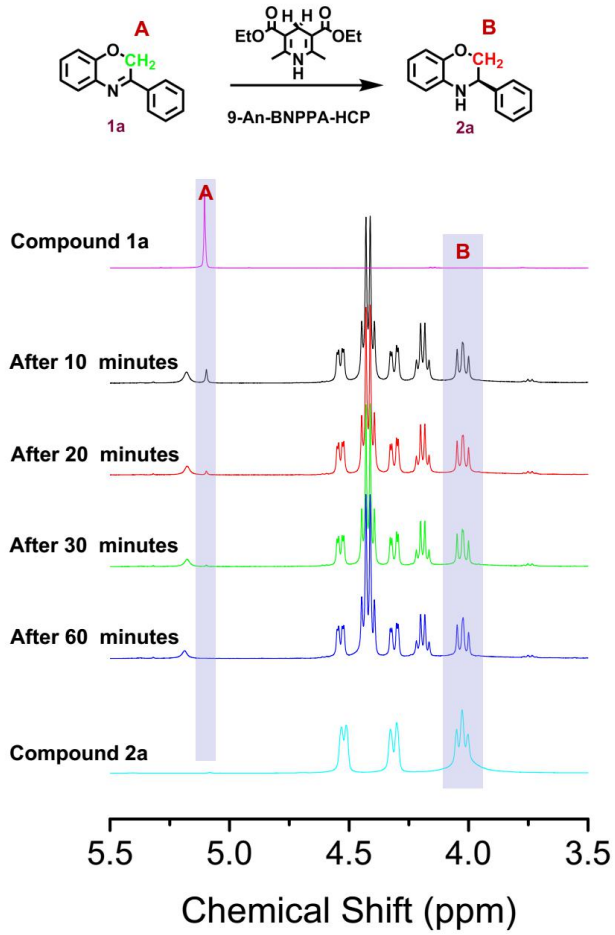

Figure S10. ^{1}H-NMR spectra of **1a**, **2a** and *in situ* NMR spectra after different reaction time. 3-Phenyl-2H-1,4-benzoxazin (10.5 mg, 0.05 mmol), Hantzsch dihydropyridine (15.8 mg, 0.6 mmol, 1.25 eq.) and the catalyst (2 mol%). $CDCl_3$ (1.5 mL) was added in 4 centrifuge vials and the mixture was stirred for 10 min, 20 min, 30 min and 60 min at 25 ^{o}C, respectively, and then the catalyst is filtered through the membrane. The filtrate was tested by NMR.

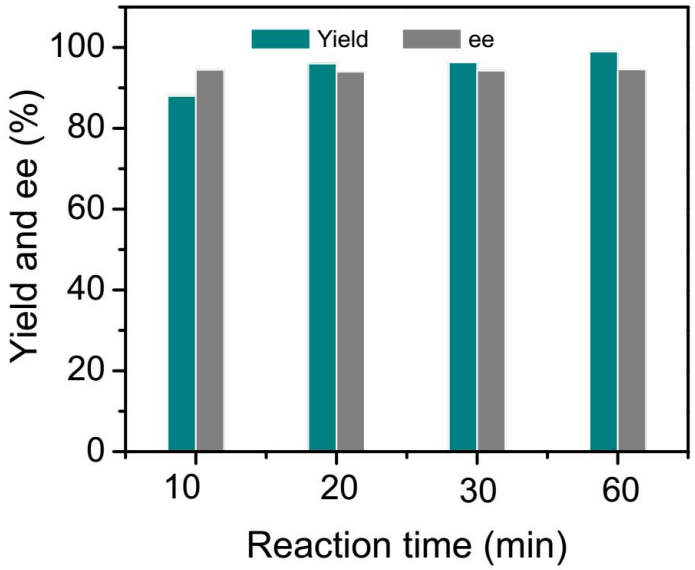

Figure S11. The effect of reaction time on the reaction performances in situ NMR experiments.

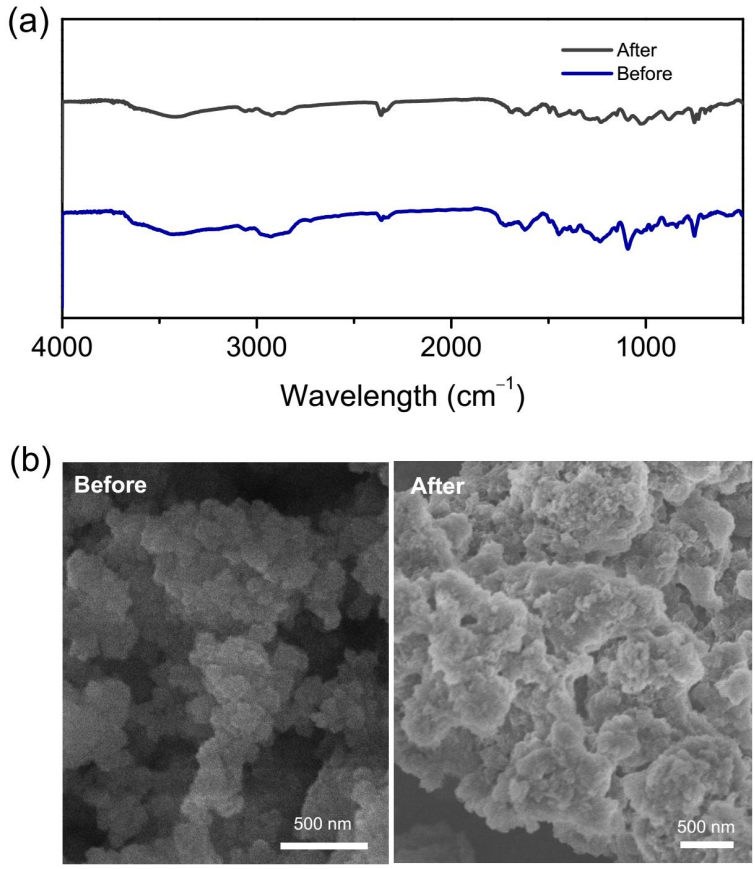

Figure S12. Reusability of 9-An-BNPPA-HCP in the asymmetric transfer hydrogenation. (a) FT-IR spectra of 9-An-BNPPA-HCP before and after ten cycles. (b) FE-SEM images of 9-An-BNPPA-HCP before and after ten cycles.

Table S1. Pore size distribution of BNPPA-HCPs on the nitrogen adsorption isotherms.

Polymers	BET surface area ($m^2\ g^{-1}$)	Langmuir surface area ($m^2\ g^{-1}$)	Total pore volume ($cm^3\ g^{-1}$)	Micropore volume ($cm^3\ g^{-1}$)
Ph-BNPPA-HCP	1098	1232	1.26	0.45
4-MeOPh-BNPPA-HCP	782	874	0.47	0.31
2-Naph-BNPPA-HCP	857	961	0.53	0.24
9-Phen-BNPPA-HCP	1026	1154	0.89	0.41
9-An-BNPPA-HCP	1001	1128	0.70	0.40

Scheme S1. Large-scale asymmetric transfer hydrogenation of 3-phenyl-1,4-benzoxazine using An-BNPPA-HCP as a heterogeneous catalyst.

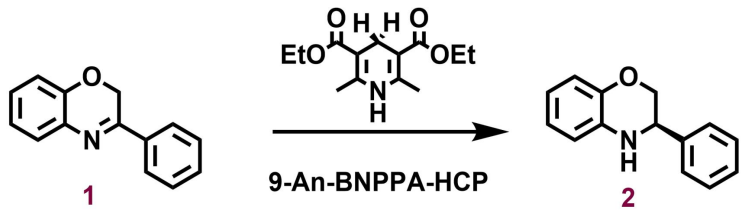

1

1.0 g

2

0.93 g
Yield: 92%
ee: 97%

A centrifuge vial was charged with 3-Phenyl-2*H*-1,4-benzoxazin (1.0 g, 4.8 mmol), Hantzsch dihydropyridine (1.52 g, 6.0 mmol, 1.25 eq.) and the catalyst (2 mol%). $CHCl_3$ (15 mL) was added and the mixture was stirred for 4 h at room temperature. In case of a homogeneous reaction the solvent was removed in vacuum. In case of a heterogeneous reaction the catalyst was separated by centrifugation. The organic layers were combined and the solvents were removed in vacuum. The yield was determined after column chromatography (SiO_2, hexane / AcOEt = 40:1), which was 0.93 g (92%) of a white solid.

Section 5. Compared with recent homogeneous catalysts

Table S2. Compared with recent homogeneous catalysts for asymmetric transfer hydrogenation.

Catalyst system	Substrate	Hydride source	Solvent	T (°C)	t (h)	Conv. (%)	Yield (%)	ee (%)
9-An-BNPPA-HCP	benzoxazines	Hantzsch dihydropyridine	$CHCl_3$	25	1	–	91-99	94-98
	benzoxazinones				24	–	88-93	97-99
	quinolines				12	–	83-98	91-99
[5a]BINOL-based polymer network	dihydro-2H-benzoxazine	Hantzsch dihydropyridine	$CHCl_3$	Rt.	24	99	–	47-56
[5b]BNPPA-derived polymer network	quinolines	Hantzsch dihydropyridine	$CHCl_3$	Rt.	4	99	–	87-98
[5c]BiCz-POF-1	3-Phenyl Benzoxazine	Hantzsch dihydropyridine	THF	Rt.	24	–	95	94
	3-Phenyl Benzoxazinone		$CHCl_3$	40	24	–	95	96
	2-Phenylquinoline		THF	40	24	–	95	90
[5d]NAD(P)H analogues (*R*)-6a/ $Sm(OTf)_3$/ $[Ru(p\text{-cymene})I_2]_2$	benzoxazinones	H_2	$CHCl_3$	50	72	–	89-98	92-98
[5e]NAD(P)H Models (*R*)-1f/Bis(4-nitrophenyl) phosphate/$[Ru(p\text{-cymene})I_2]_2$	benzoxazinones	H_2	$CHCl_3$	40	22	–	83-97	92-99
	benzoxazine		$CHCl_3$	40	48	–	85	91
	quinolines		$CHCl_3$/THF 3/1	40	48	–	94-99	83-90
[5f](*S*)-3,3'-Diaryl-1,1'-binaphthyl phosphate	benzoxazines	4,5-dihydropyrrolo[1,2-a]quinoxalines	THF/benzene 2/1	40	38	–	87-96	84-92
[5g]Bisborane adducts	quinolines	H_2	$PhCF_3$	-20	24	–	63-99	87-99
5hBisphosphine ligand/$Pd(OCOCF_3)_2$	quinolines	H_2	CH_2Cl_2	70/80	18	–	72-99	79-90
[5i]Ferrocene–thiourea chiral bisphosphine ligand/ $[Rh(COD)Cl]_2$	quinolines	H_2	DCM/iPrOH 2/1	25	48	–	73-99	91-99
[5j]SPIROL-based diphosphinite ligands (SPIRAPO)/ $[Ir(COD)Cl]_2$	quinolines	H_2	THF	Rt.	10	–	79-99	86-96
	benzoxazinones					–	95-99	73-85
[5k](*S*)-SegPhos/$[Ir(COD)Cl]_2$	benzoxazine	H_2	benzene	Rt.	15	–	91-98	84-92
[5l]Mn^I model/ planar-chiral ferrocene-based NAD(P) analogue/ $La(OTf)_3$	benzoxazines	H_2	$CHCl_3$	80	48	–	74-85	71-88
	benzoxazinones					–	58-90	82-96
[5m](*R*,*R*)-Ru-catalyst	quinolines	H_2	iPrOH	25	24	–	89-95	94-98
[5n](*R*,*R*)-Ru-MsDPEN	benzoxazines	H_2	toluene	40	12	–	94-98	82-98
[5o](+)-Xyl-P16C6-Phos/ $[Ir(COD)_2]BF_4$/ $NaBAr_F$	quinolines	H_2	ethyl acetate	Rt.	24	–	96-98	90-97

Section 6. NMR and HPLC Spectra of Catalytic Products

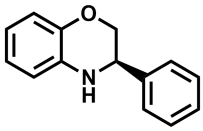

^{1}H NMR (400 MHz, $CDCl_3$) δ: 7.43 (m, 5H), 6.90-6.83 (m, 2H), 6.76-6.69 (m, 2H), 4.53 (d, *J* = 8.0 Hz, 1H), 4.33 (d, *J* =12.0 Hz, 1H), 4.05 (m, 2H) ppm. ^{13}C NMR (100 MHz, $CDCl_3$) δ: 143.65, 139.31, 134.05, 128.93, 128.44, 127.33, 121.61, 119.03, 116.72, 115.53, 71.23, 71.03, 54.30 ppm. HPLC conditions: Chiracel OD-H, n-hexane/2-propanol = 80/20, flow rate = 1 mL min^{-1}, major enantiomer: t_R = 10.63 min; minor enantiomer: t_R = 14.86 min.

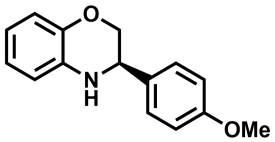

^{1}H NMR (400 MHz, $CDCl_3$) δ: 7.36-7.29 (d, *J* = 8.0 Hz, 2H), 6.93-6.91 (d, *J* = 8.0 Hz, 2H), 6.86-6.79 (m, 1H), 6.72-6.66 (m, 1H), 4.48-4.43 (m, 1H), 3.99-3.95 (m,1H), 3.82 ppm (s, 3H) ppm. ^{13}C NMR (100 MHz, $CDCl_3$) δ: 159.66, 143.53, 136.10, 131.16, 128.33, 121.44, 118.90, 116.58, 115.35, 114.23, 71.12, 55.35, 53.61 ppm. HPLC conditions: Chiracel OD-H, n-hexane/2-propanol = 80/20, flow rate = 1mL min^{-1}, major enantiomer: t_R = 11.12 min; minor enantiomer: t_R = 18.16 min.

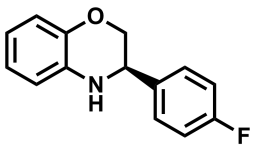

^{1}H NMR (400 MHz, $CDCl_3$) δ: 7.40 (m, 2H), 7.10-7.06 (m, 2H), 6.87-6.80 (m, 2H), 6.73-6.67 (m, 2H), 4.51 (d, *J* = 8.0 Hz,1H), 4.27 (d, *J* = 8.0Hz,1H), 3.99-3.94 (m, 2H) ppm. ^{13}C NMR (100 MHz, $CDCl_3$) δ: 163.91, 161.46, 143.54, 135.03, 133.76, 128.81, 119.13, 116.67, 115.87, 115.65, 115.48, 70.93, 53.55 ppm. HPLC conditions: Chiracel OD-H, n-hexane/2-propanol = 80/20, flow rate=0.6 mL min^{-1}, major enantiomer: t_R = 10.30 min; minor enantiomer: t_R = 17.36 min.

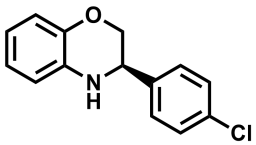

^{1}H NMR (400 MHz, $CDCl_3$,) δ: 7.38-7.34 (m, 4H), 6.81-6.81 (m, 2H), 6.74-6.68 (m, 2H), 4.51 (d, *J* = 8.0Hz,1H), 4.24 (d, *J* = 8.0 Hz, 1H), 3.99-3.94 (m, 2H) ppm. ^{13}C NMR (100 MHz, $CDCl_3$,) δ: 143.52, 137.79, 134.10, 133.62, 129.04, 128.56, 121.65, 119.18, 116.70, 115.51, 70.74, 53.63, 161.46, 143.62, 128.81, 119.13, 116.67, 115.87, 115.65, 115.48, 70.93, 53.55 ppm. HPLC conditions: Chiracel OD-H, n-hexane/2-propanol = 80/20, flow rate = 0.6 mL min^{-1}, major enantiomer: t_R = 12.22 min; minor enantiomer: t_R = 24.00 min.

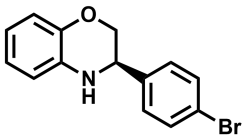

^{1}H NMR (400 MHz, $CDCl_3$,) δ: 7.42 (m, 4H), 6.89-6.82 (m, 2H), 6.74-6.68 (m, 2H), 4.53 (d, *J* = 8.0 Hz, 1H), 4.32 (d, *J* = 8.0 Hz, 1H), 4.04-3.99 (m, 2H) ppm. ^{13}C NMR (100 MHz, $CDCl_3$) δ*:* 143.50, 138.31, 131.98, 128.86, 122.18, 121.57, 119.19, 116.68, 115.46, 70.71, 53.68 ppm. HPLC conditions: Chiracel OD-H, n-hexane/2-propanol = 80/20, flow rate = 1 mL min^{-1}, major enantiomer: t_R = 13.36 min; minor enantiomer: t_R = 26.28 min.

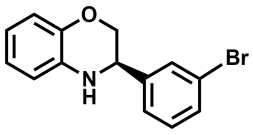

^{1}H NMR (400 MHz, $CDCl_3$,) δ: 7.60-7.59 (m, 1H), 7.51-7.49 (m, 1H), 7.37-7.35 (m, 1H), 7.30-7.28 (m, 1H), 6.89-6.83 (m, 2H), 6.77-6.70 (m, 2H), 4.53-4.50 (m, 1H), 4.32-4.28 (m, 1H), 4.02-3.97 (m, 2H) ppm. ^{13}C NMR (100 MHz, $CDCl_3$) δ*:* 143.51, 141.67, 131.47, 130.45, 130.31, 125.97, 123.00, 121.72, 119.25, 116.74, 115.59, 70.68, 53.79 ppm. HPLC conditions: Chiracel OD-H, n-hexane/2-propanol = 80/20, flow rate = 1 mL min^{-1}, major enantiomer: t_R = 12.94 min; minor enantiomer: t_R = 19.19 min.

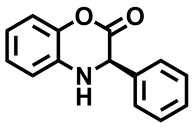

^{1}H NMR (400 MHz, $CDCl_3$,) δ: 7.43-7.34 (m, 5H), 7.07-7.01 (m, 2H), 6.90-6.81 (m, 2H), 5.08 (s, 1H), 4.22 (br s, 1H) ppm. ^{13}C NMR (100 MHz, $CDCl_3$) δ*:* 165.12, 140.94, 136.36, 132.34, 129.02, 127.49, 125.17, 120.45, 117.02, 114.84, 59.32 ppm. HPLC conditions: Chiracel OD-H, n-hexane/2-propanol = 80/20, flow rate = 1 mL min^{-1}, major enantiomer: t_R = 11.79 min; minor enantiomer: t_R = 17.66 min.

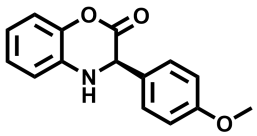

^{1}H NMR (400 MHz, $CDCl_3$,) δ: 7.33-7.31 (m, 2H), 7.05-7.00 (m, 2H), 6.90-6.79 (m, 4H), 4.99 (s, 1H), 4.22 (br s, 1H), 3.79 (s, 1H) ppm. ^{13}C NMR (100 MHz, $CDCl_3$) δ*:* 165.54, 160.74, 141.00, 132.58, 128.79, 128.40, 125.14, 120.36, 116.97, 114.87, 114.39, 58.81, 55.33 ppm; HPLC conditions: Chiracel OD-H, n-hexane/2-propanol=80/20, flow rate=1 mL min^{-1}, major enantiomer: t_R = 14.02 min; minor enantiomer: t_R = 40.33 min.

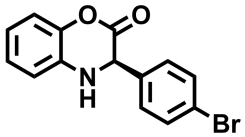

^{1}H NMR (400 MHz, $CDCl_3$,) δ: 7.48-7.45 (m, 2H), 7.40-7.37 (m, 2H), 6.73-6.70 (m, 2H), 6.64-6.60 (m, 1H), 6.38 (d, *J* = 8.0Hz, 1H), 5.04 (br s, 1H) ppm. ^{13}C NMR (100 MHz, $CDCl_3$) δ*:* 171.66, 144.06, 136.88, 134.57, 131.97, 128.94, 122.47, 121.47, 118.89, 114.70, 113.46, 62.07, 60.88 ppm. HPLC conditions: Chiracel OD-H, n-hexane/2-propanol = 80/20, flow rate = 1 mL min^{-1}, major enantiomer: t_R = 19.23 min; minor enantiomer: t_R = 41.66 min.

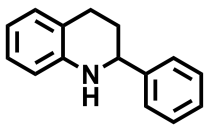

^{1}H NMR (400 MHz, $CDCl_3$) δ: 7.47-7.34 (m, 5H), 7.11-7.07 (m, 2H), 6.75-6.59 (m, 2H), 6.57-6.55 (m, 1H, Ar-H), 4.52-4.49 (m, 1H), 4.04 (s, 1H), 3.04-2.78 (m, 2H), 2.23-2.02 (m, 2H) ppm. ^{13}C NMR (100 MHz, $CDCl_3$) δ*:* 144.86, 144.76, 128.62, 126.95, 126.59, 120.91, 117.20, 114.03, 56.30, 31.03, 26.43 ppm. HPLC conditions: Chiracel OD-H, n-hexane/2-propanol = 80/20, flow rate = 1 mL min^{-1}, major enantiomer: t_R = 8.37 min; minor enantiomer: t_R = 11.07 min.

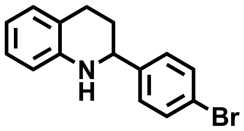

^{1}H NMR (400 MHz, $CDCl_3$,) δ: 7.48-7.46 (m, 2H), 7.28-7.25 (m, 2H), 7.04-7.00 (m, 2H), 6.69-6.65 (m, 1H), 6.57-6.55 (m, 1H), 4.43-4.40 (m, 2H), 3.97 (br s, 1H), 2.95-2.87 (m, 1H), 2.75-2.68 (m, 1H), 2.13-2.07 (m, 1H), 2.00-1.90 (m, 1H) ppm. ^{13}C NMR (100 MHz, $CDCl_3$) δ*:* 165.53, 160.07, 141.00, 132.58, 128.79, 128.14, 125.14, 120.36, 116.97, 114.87, 114.39, 58.81, 55.33 ppm. HPLC conditions: Chiracel OD-H, n-hexane/2-propanol = 80/20, flow rate = 1 mL min^{-1}, major enantiomer: t_R = 10.33 min; minor enantiomer: t_R = 19.33 min.

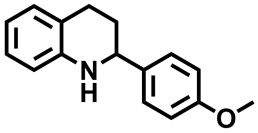

^{1}H NMR (400 MHz, $CDCl_3$,) δ: 7.33 (d, *J* = 8.0 Hz, 2H), 7.01 (m, 2H), 6.91 (d, *J* = 8.0 Hz, 2H), 6.67-6.64 (m, 2H), 6.54 (d, *J* = 8.0 Hz, 2H), 4.40 (d, *J* = 8.0 Hz, 1H), 3.82 (s, 3H), 2.98-2.73 (m, 2H), 2.11-1.93 (m, 2H) ppm. ^{13}C NMR (100 MHz, $CDCl_3$) δ*:* 158.98, 144.84, 136.91, 129.30, 127.65, 126.87, 120.89, 117.13, 113.97, 113.94, 55.74, 55.33, 31.11, 26.57 ppm. HPLC conditions: Chiracel OD-H, n-hexane/2-propanol = 80/20, flow rate = 1 mL min^{-1}, major enantiomer: t_R = 8.50 min; minor enantiomer: t_R = 13.60 min.

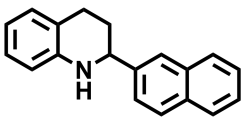

^{1}H NMR (400 MHz, $CDCl_3$,) δ: 7.92-7.88 (m, 4H), 7.60-7.52 (m, 3H), 7.14-7.09 (m, 2H), 6.78-6.74 (m, 1H), 6.66 (d, *J* = 8.0 Hz, 1H), 4.68-4.64 (m, 1H), 4.14 (br s, 1H), 3.07-2.99 (m, 1H), 2.87-2.80 (m, 1H), 2.29-2.11 (m, 2H) ppm. ^{13}C NMR (100 MHz, $CDCl_3$) δ*:* 144.75, 142.28, 133.48, 133.02, 129.38, 127.91, 127.74, 127.01, 126.21, 125.82, 125.15, 124.92, 121.01, 117.29, 114.10, 56.40, 31.00, 26.47 ppm. HPLC conditions: Chiracel OD-H, n-hexane/2-propanol = 80/20, flow rate = 1 mL min^{-1}, major enantiomer: t_R = 12.22 min; minor enantiomer: t_R = 22.08 min.

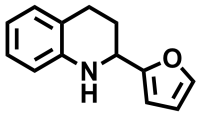

^{1}H NMR (400 MHz, $CDCl_3$) δ: 7.39-7.38 (m, 1H), 7.03-6.98 (m, 2H), 6.68-6.65 (m, 1H), 6.57-6.55 (m, 1H), 6.35-6.34 (m, 1H), 6.22-6.21 (m, 1H), 4.56-4.53 (m, 1H), 4.13 (br s, 1H), 2.92-2.84 (m, 1H), 2.80-2.73 (m, 1H), 2.26-2.10 (m, 2H) ppm. ^{13}C NMR (100 MHz, $CDCl_3$) δ: 156.96, 143.76, 141.62, 129.27, 126.89, 120.97, 117.56, 114.35, 110.18, 105.21, 49.70, 26.92, 25.54 ppm. HPLC conditions: Chiracel OD-H, n-hexane/2-propanol = 80/20, flow rate = 1 mL min^{-1}, major enantiomer: t_R = 7.09 min; minor enantiomer: t_R = 7.69 min.

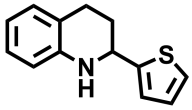

^{1}H NMR (400 MHz, $CDCl_3$) δ: 7.29-7.28 (m, 1H), 7.11-7.06 (m, 4H), 6.80-6.76 (m, 1H), 6.63(d, *J* = 12.0 Hz, 1H), 4.84-4.81 (m, 1H), 4.21 (br s, 1H), 3.06-2.85 (m, 2H) ppm. ^{13}C NMR (100 MHz, $CDCl_3$) δ: 149.02, 144.08, 129.37, 127.00, 126.74, 124.15, 123.64, 120.98, 117.76, 114.41, 52.06, 31.90, 26.24 ppm. HPLC conditions: Chiracel OD-H, n-hexane/2-propanol = 80/20, flow rate = 1 mL min^{-1}, major enantiomer: t_R = 10.91 min; minor enantiomer: t_R = 14.64 min.

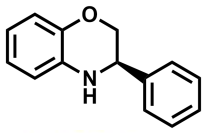
O
N
H

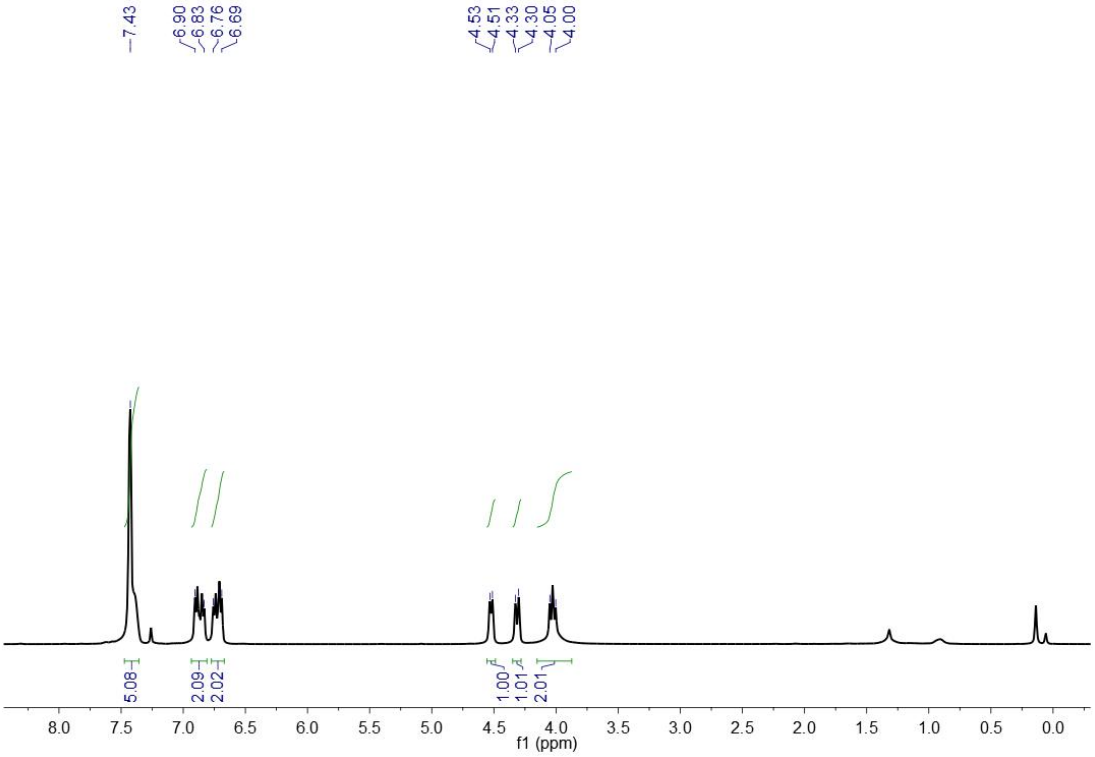
7.43
6.90
6.83
6.76
6.69
4.53
4.51
4.33
4.30
4.05
4.00
5.08
2.09
2.02
1.00
1.01
2.01
8.0 7.5 7.0 6.5 6.0 5.5 5.0 4.5 4.0 3.5 3.0 2.5 2.0 1.5 1.0 0.5 0.0
f1 (ppm)

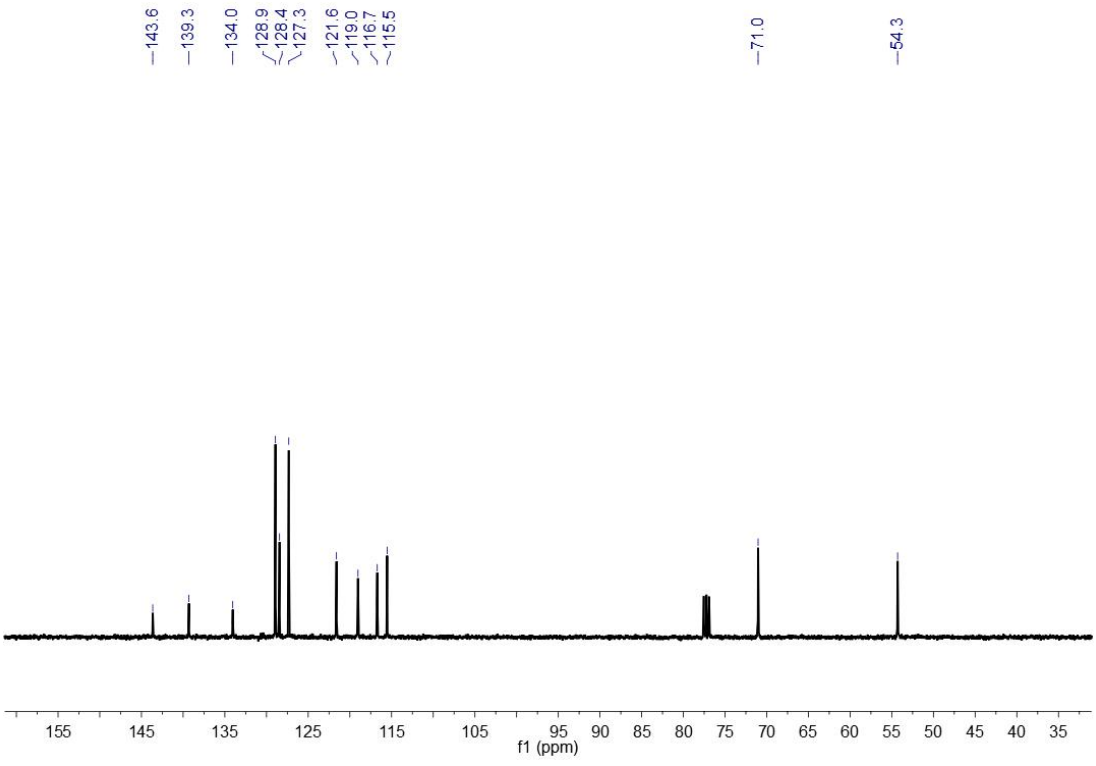
143.6
139.3
134.0
128.9
128.4
127.3
121.6
119.0
116.7
115.5
71.0
54.3
155 145 135 125 115 105 95 90 85 80 75 70 65 60 55 50 45 40 35
f1 (ppm)

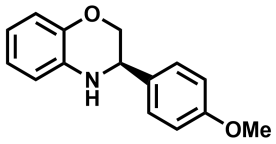
O
N
H
OMe

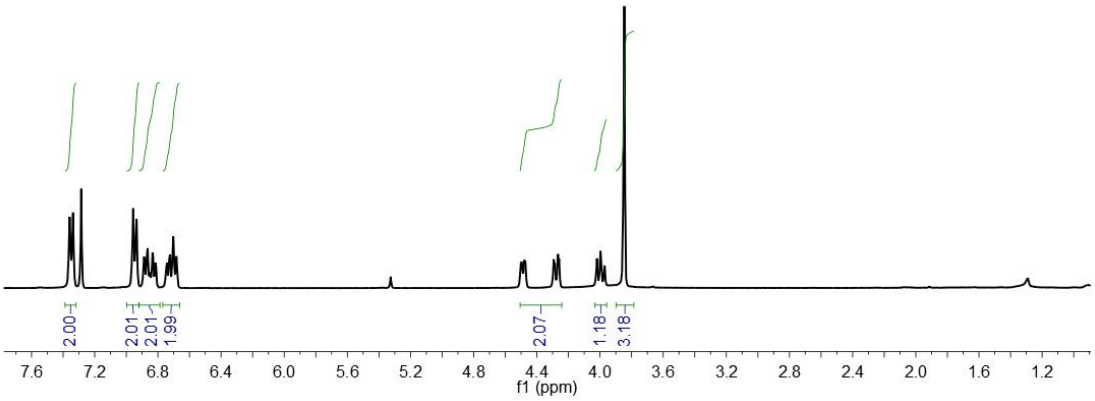
2.00
2.01
2.01
1.99
2.07
1.18
3.18
7.6
7.2
6.8
6.4
6.0
5.6
5.2
4.8
4.4
4.0
3.6
3.2
2.8
2.4
2.0
1.6
1.2
f1 (ppm)

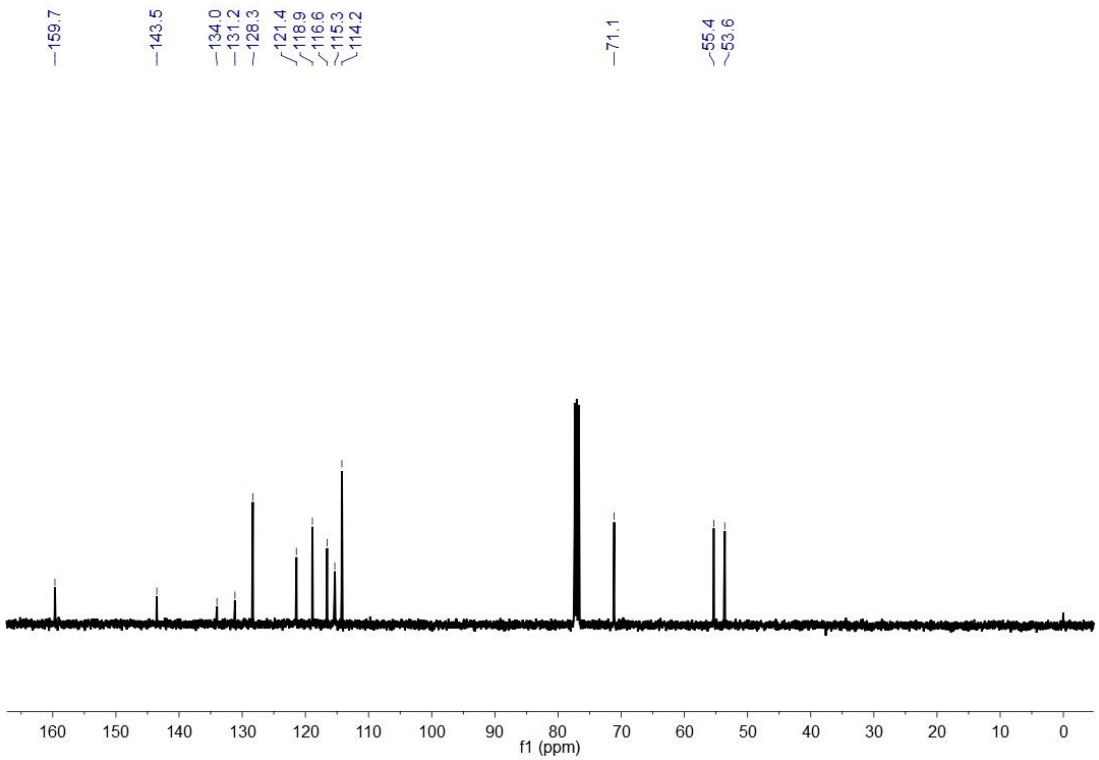
159.7
143.5
134.0
131.2
128.3
121.4
118.9
116.6
115.3
114.2
71.1
55.4
53.6
160 150 140 130 120 110 100 90 80 70 60 50 40 30 20 10 0
f1 (ppm)

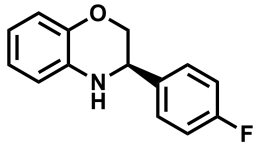
O
N
H
F

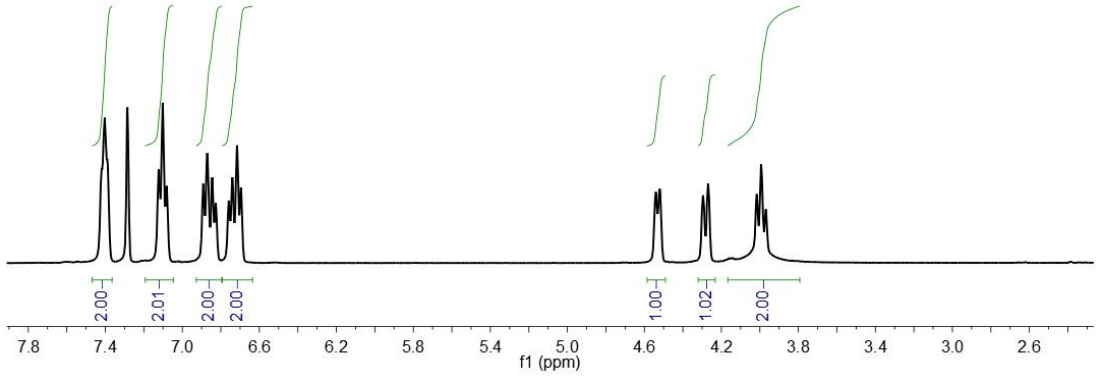
2.00
2.01
2.00
2.00
1.00
1.02
2.00
7.8 7.4 7.0 6.6 6.2 5.8 5.4 5.0 4.6 4.2 3.8 3.4 3.0 2.6
f1 (ppm)

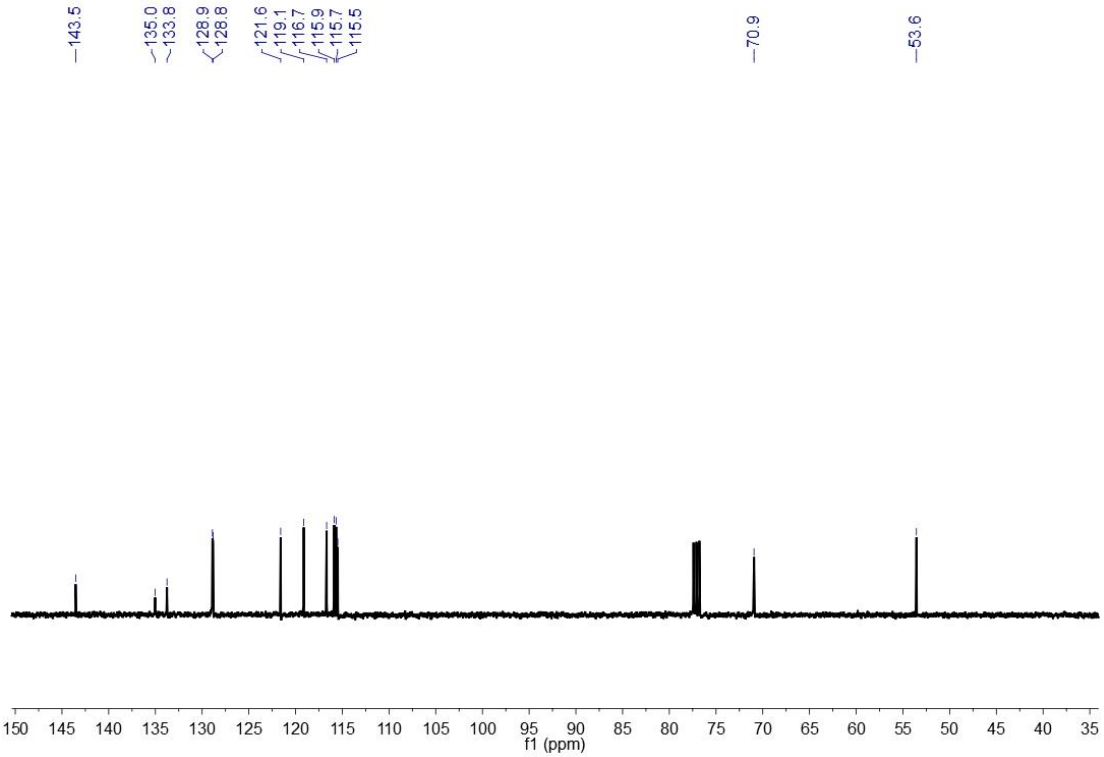
143.5
135.0
133.8
128.9
128.8
121.6
119.1
116.7
115.9
115.7
115.5
70.9
53.6
150 145 140 135 130 125 120 115 110 105 100 95 90 85 80 75 70 65 60 55 50 45 40 35
f1 (ppm)

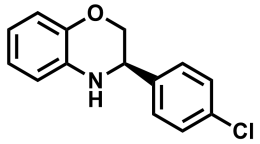
O
N
H
Cl

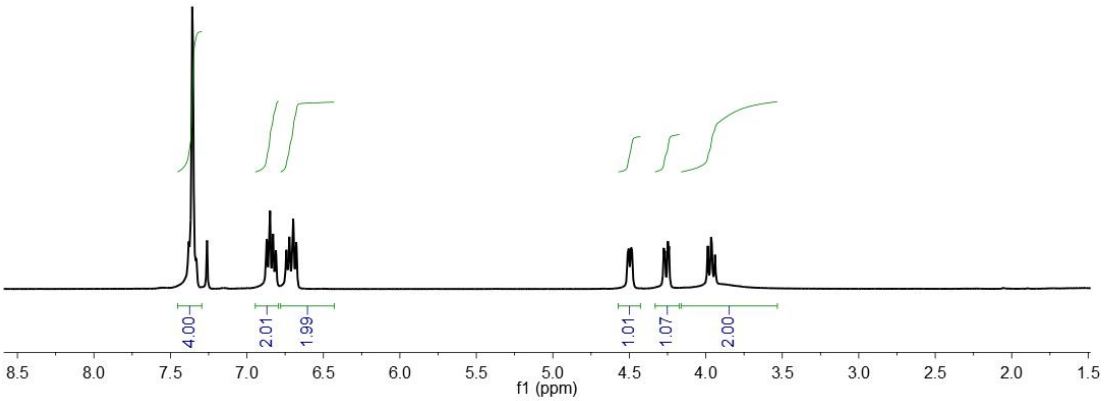
4.00
2.01
1.99
1.01
1.07
2.00
8.5 8.0 7.5 7.0 6.5 6.0 5.5 5.0 4.5 4.0 3.5 3.0 2.5 2.0 1.5
f1 (ppm)

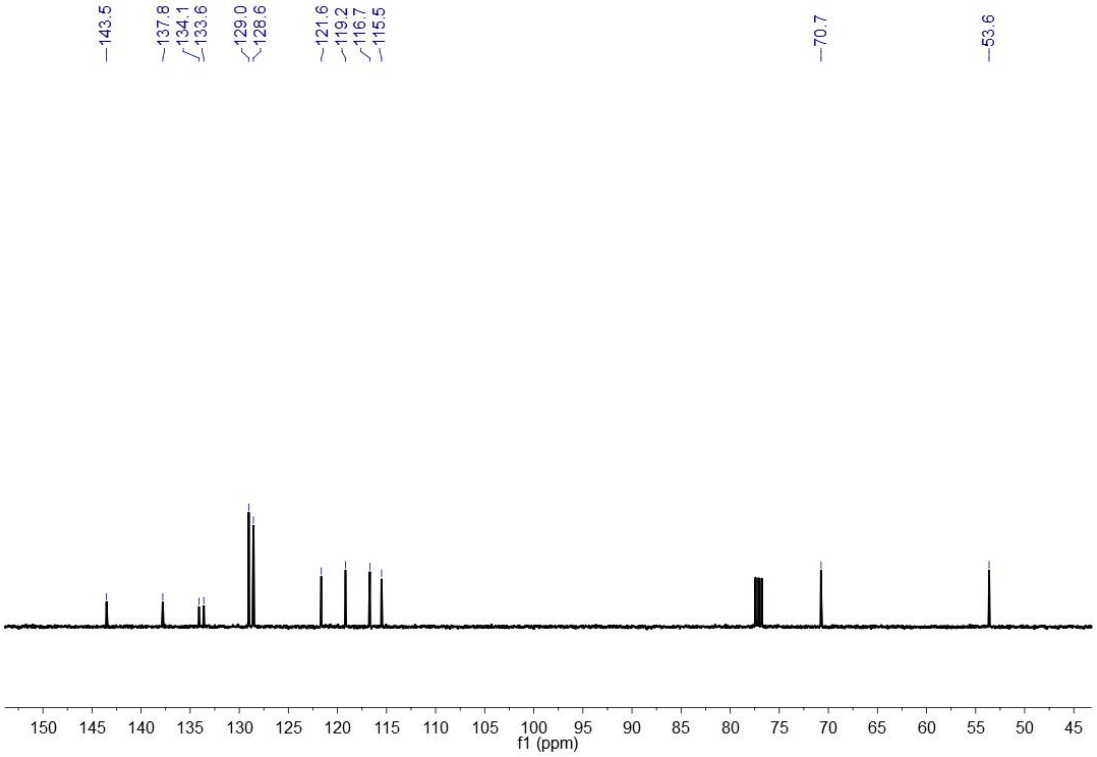
143.5
137.8
134.1
133.6
129.0
128.6
121.6
119.2
116.7
115.5
70.7
53.6
150 145 140 135 130 125 120 115 110 105 100 95 90 85 80 75 70 65 60 55 50 45
f1 (ppm)

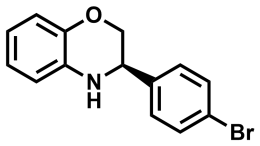
O
N
H
Br

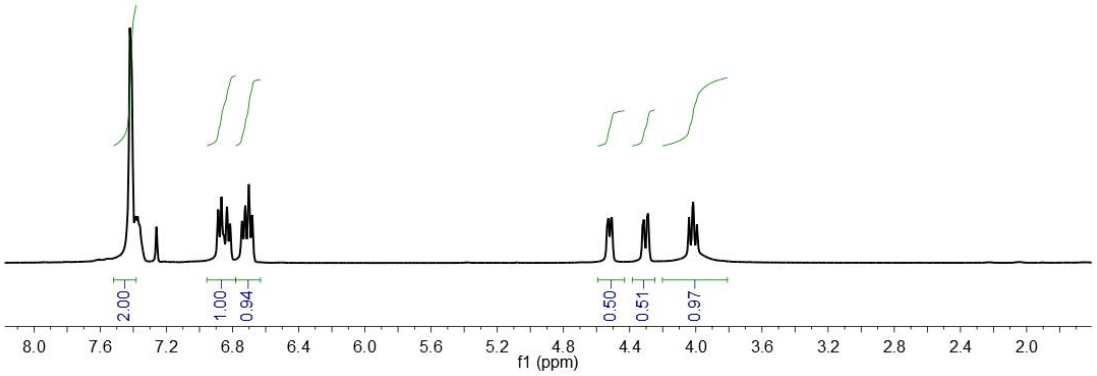
2.00
1.00
0.94
0.50
0.51
0.97
8.0 7.6 7.2 6.8 6.4 6.0 5.6 5.2 4.8 4.4 4.0 3.6 3.2 2.8 2.4 2.0
f1 (ppm)

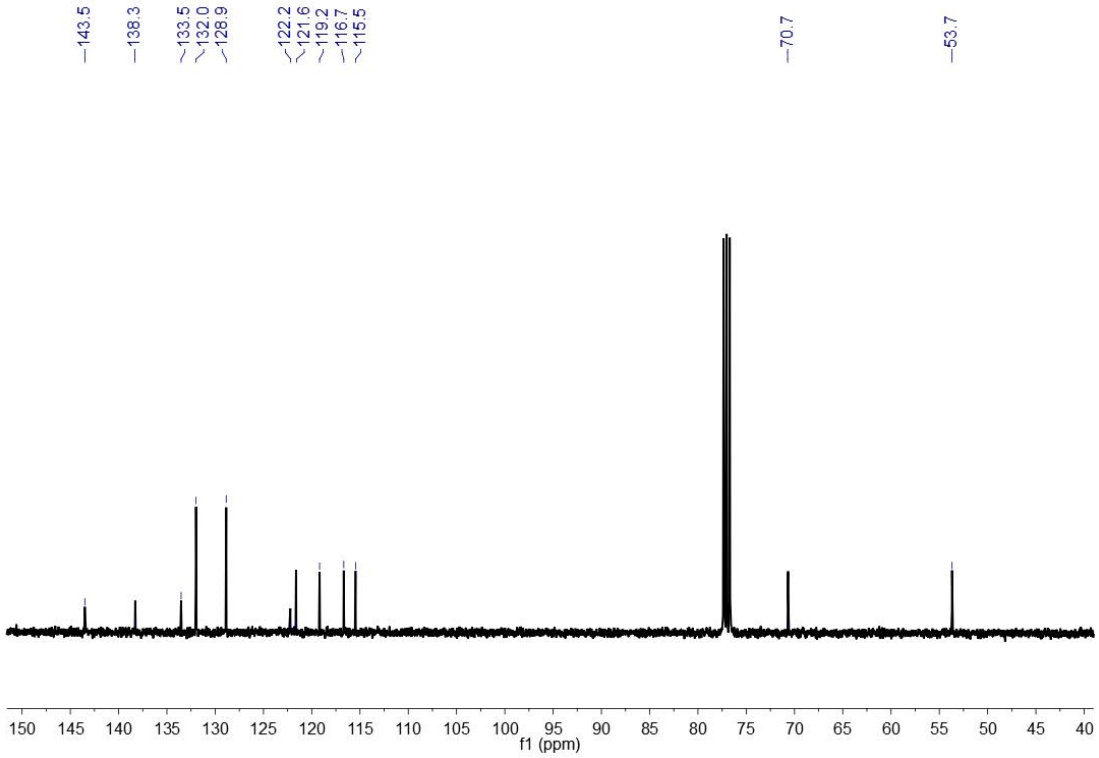
143.5
138.3
133.5
132.0
128.9
122.2
121.6
119.2
116.7
115.5
70.7
53.7
150 145 140 135 130 125 120 115 110 105 100 95 90 85 80 75 70 65 60 55 50 45 40
f1 (ppm)

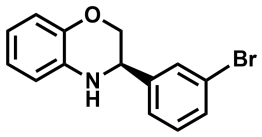
O
N
H
Br

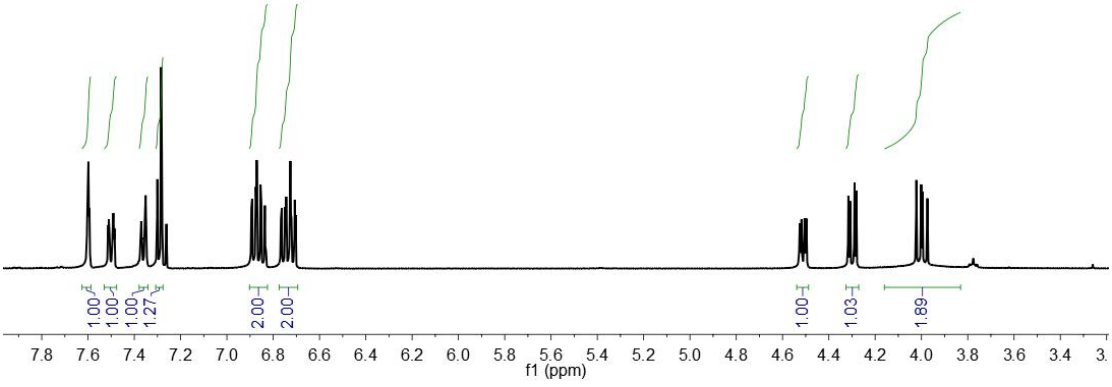
1.00
1.00
1.00
1.27
2.00
2.00
1.00
1.03
1.89
7.8 7.6 7.4 7.2 7.0 6.8 6.6 6.4 6.2 6.0 5.8 5.6 5.4 5.2 5.0 4.8 4.6 4.4 4.2 4.0 3.8 3.6 3.4
f1 (ppm)

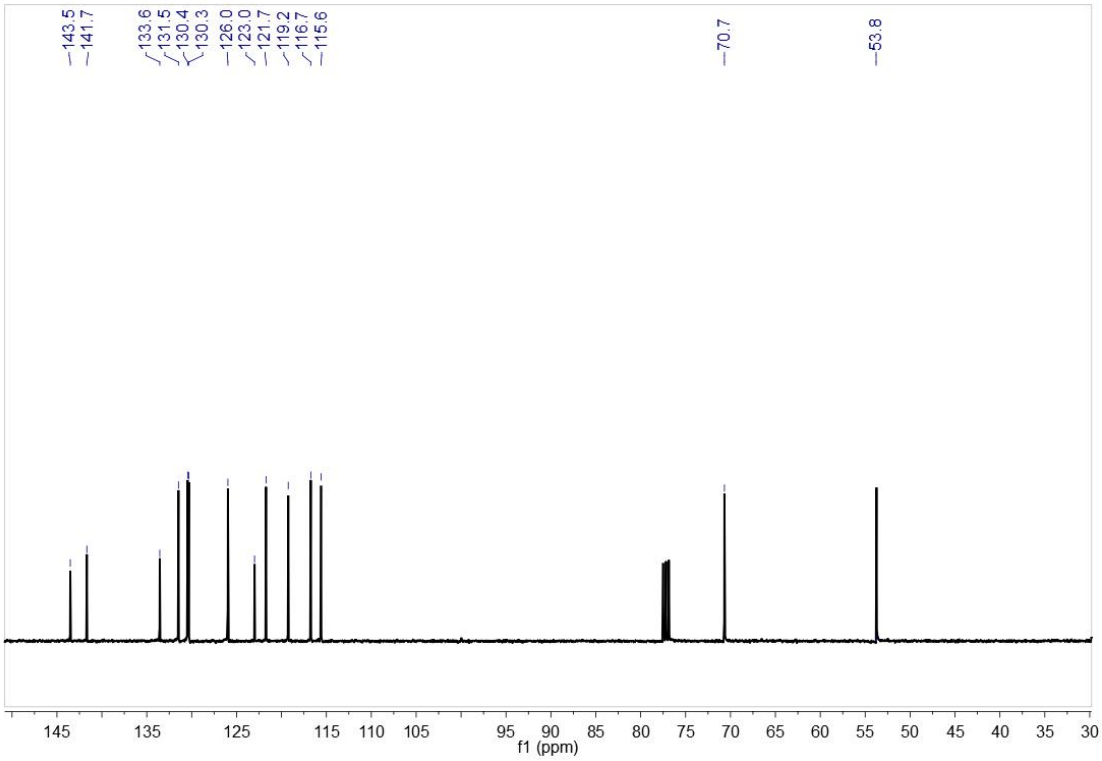
143.5
141.7
133.6
131.5
130.4
130.3
126.0
123.0
121.7
119.2
116.7
115.6
70.7
53.8
145
135
125
115
110
105
95
90
85
80
75
70
65
60
55
50
45
40
35
30
f1 (ppm)

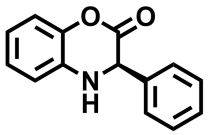
O
O
N
H

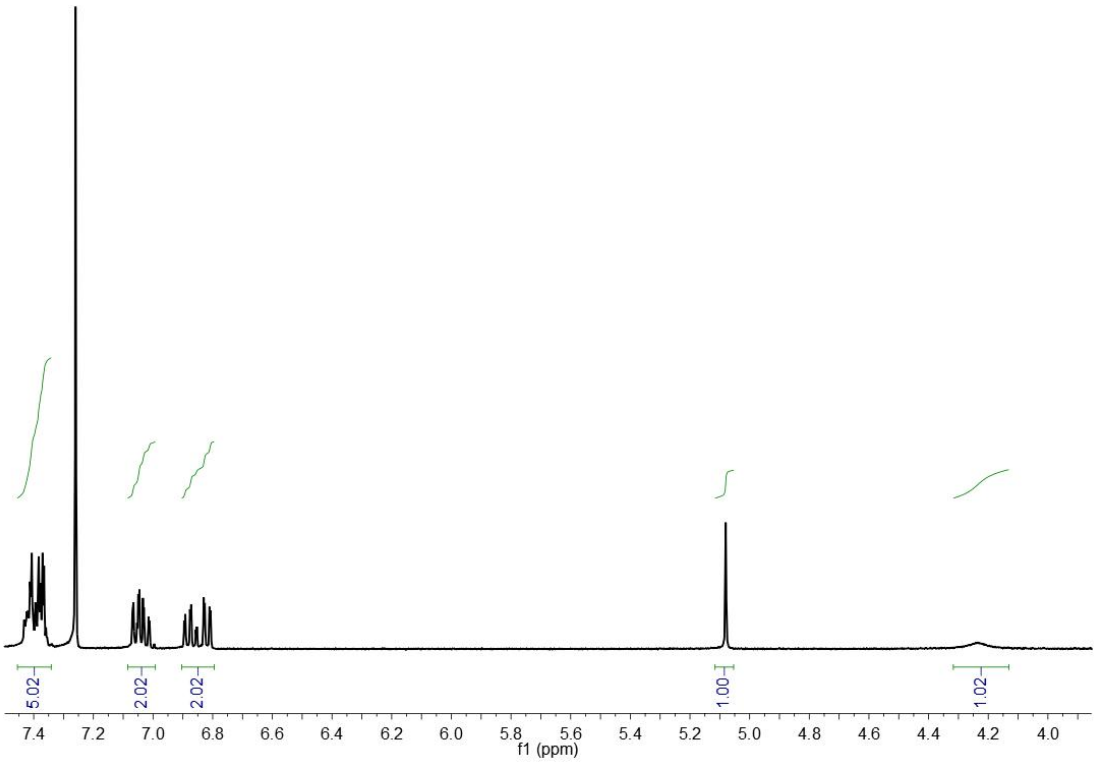
5.02
2.02
2.02
1.00
1.02
7.4
7.2
7.0
6.8
6.6
6.4
6.2
6.0
5.8
5.6
5.4
5.2
5.0
4.8
4.6
4.4
4.2
4.0
f1 (ppm)

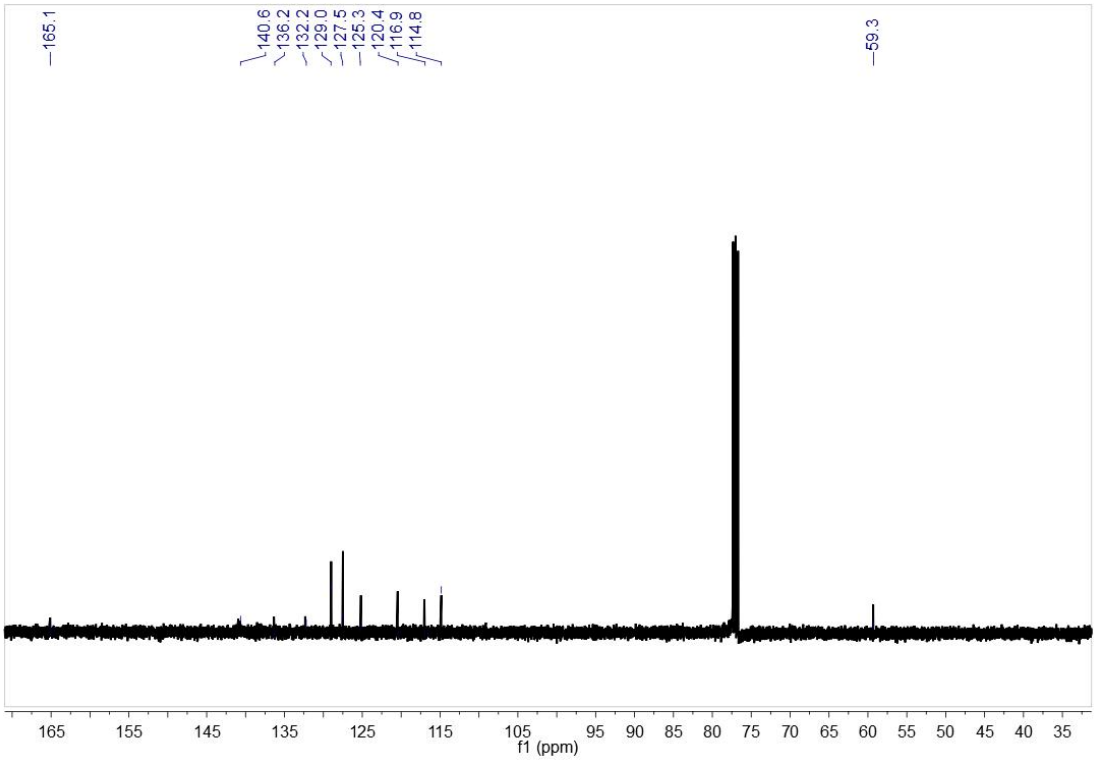
165.1
140.6
136.2
132.2
129.0
127.5
125.3
120.4
116.9
114.8
59.3
165 155 145 135 125 115 105 95 90 85 80 75 70 65 60 55 50 45 40 35
f1 (ppm)

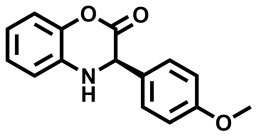
O
O
N
H
O

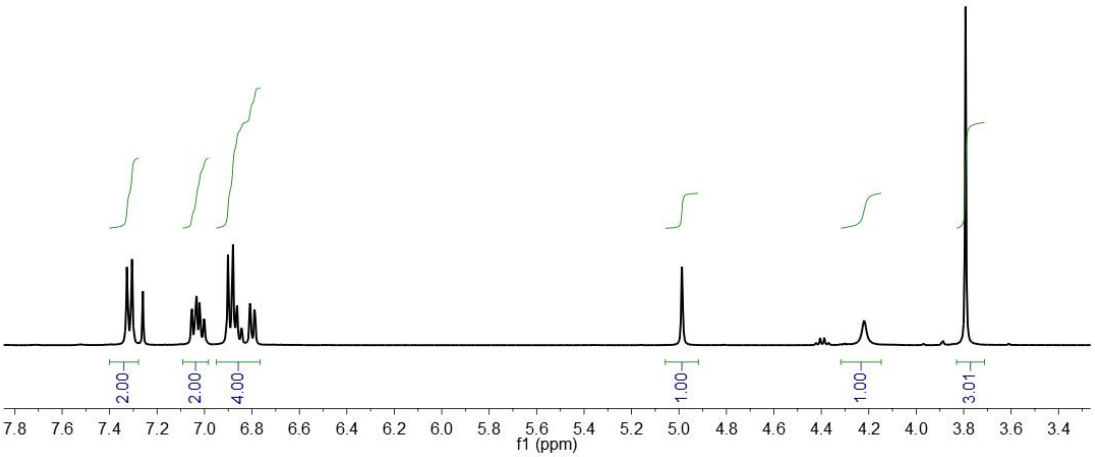
2.00
2.00
4.00
1.00
1.00
3.01
7.8 7.6 7.4 7.2 7.0 6.8 6.6 6.4 6.2 6.0 5.8 5.6 5.4 5.2 5.0 4.8 4.6 4.4 4.2 4.0 3.8 3.6 3.4
f1 (ppm)

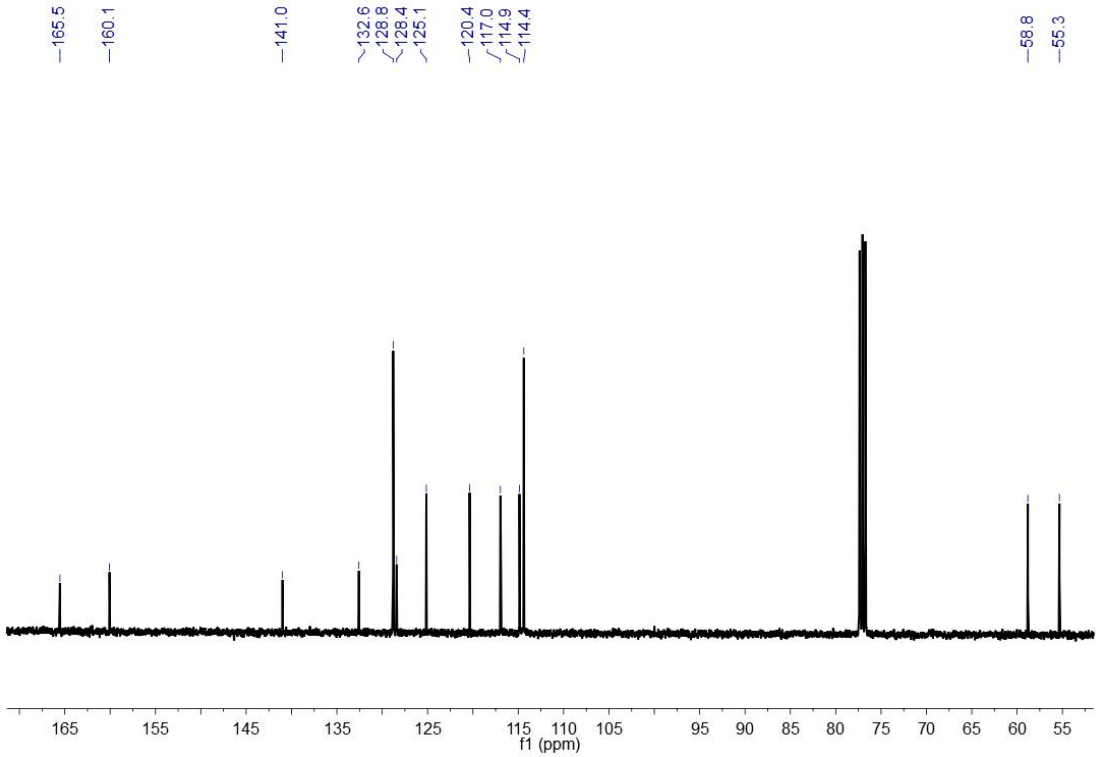
165.5
160.1
141.0
132.6
128.8
128.4
125.1
120.4
117.0
114.9
114.4
58.8
55.3
165
155
145
135
125
115
110
105
95
90
85
80
75
70
65
60
55
f1 (ppm)

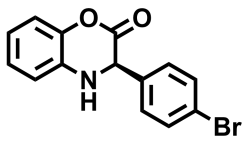
O
O
N
H
Br

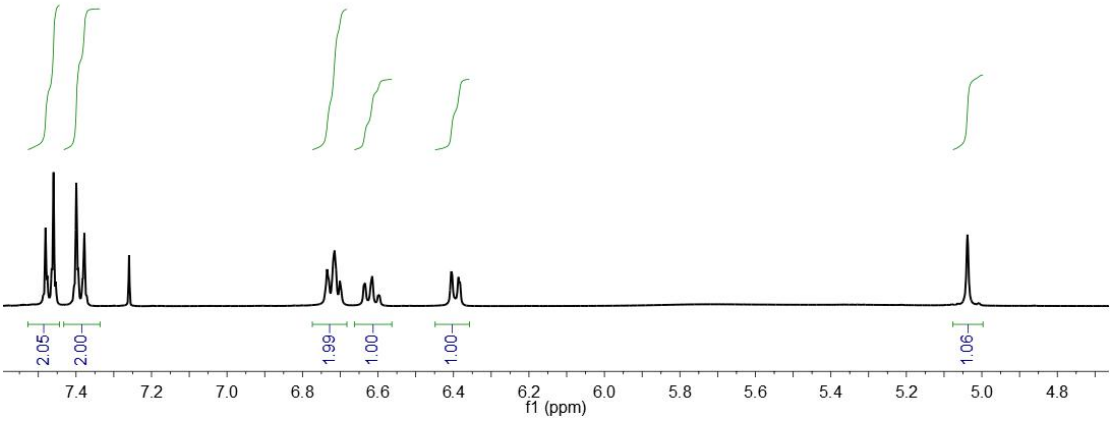
2.05
2.00
1.99
1.00
1.00
1.06
7.4
7.2
7.0
6.8
6.6
6.4
6.2
6.0
5.8
5.6
5.4
5.2
5.0
4.8
f1 (ppm)

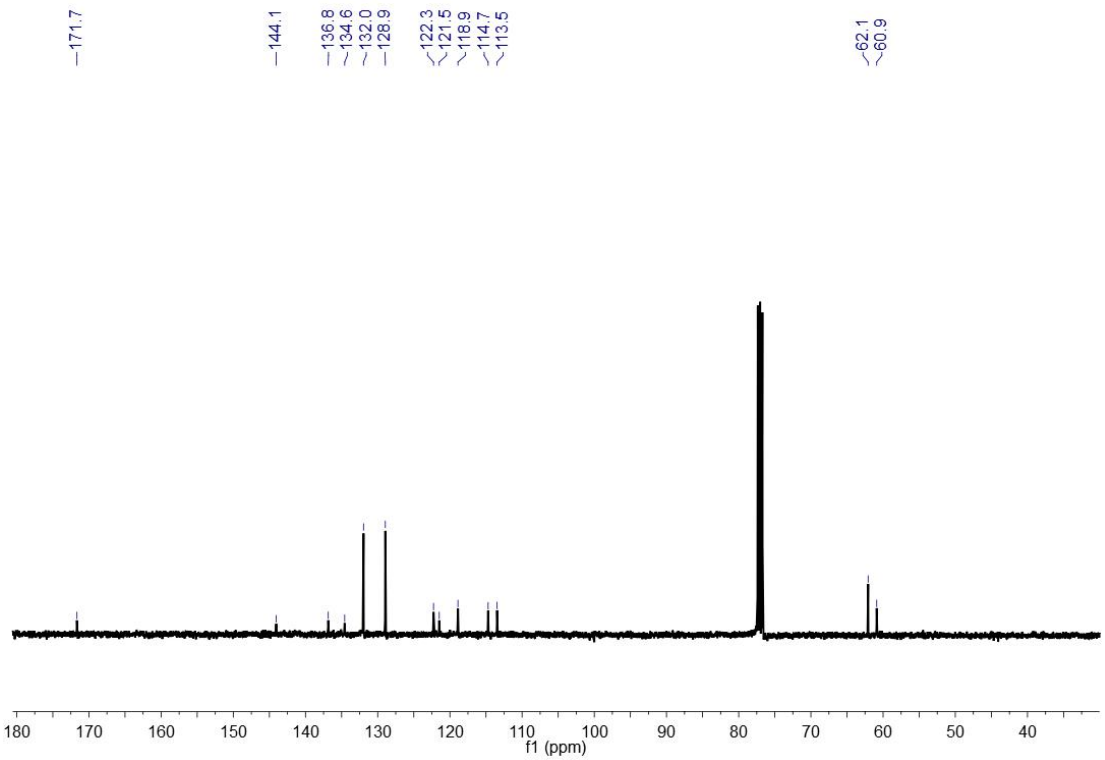
171.7
144.1
136.8
134.6
132.0
128.9
122.3
121.5
118.9
114.7
113.5
62.1
60.9
180 170 160 150 140 130 120 110 100 90 80 70 60 50 40
f1 (ppm)

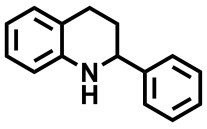
N
H

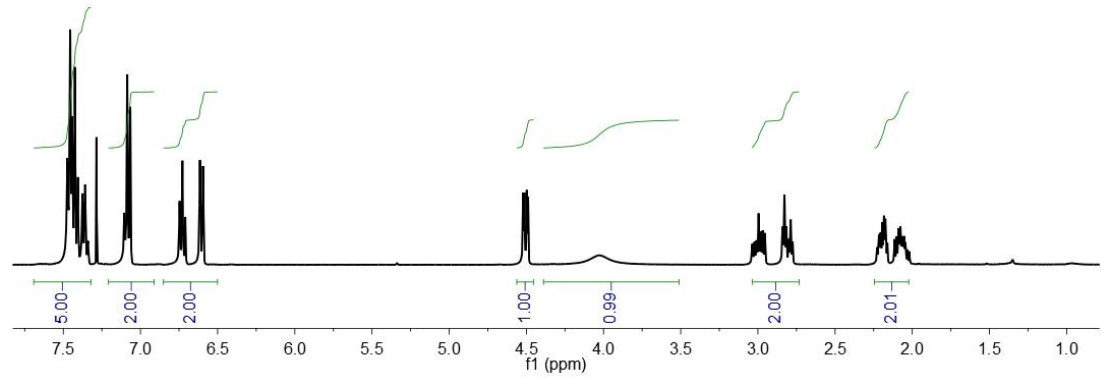
5.00
2.00
2.00
1.00
0.99
2.00
2.01
7.5 7.0 6.5 6.0 5.5 5.0 4.5 4.0 3.5 3.0 2.5 2.0 1.5 1.0
f1 (ppm)

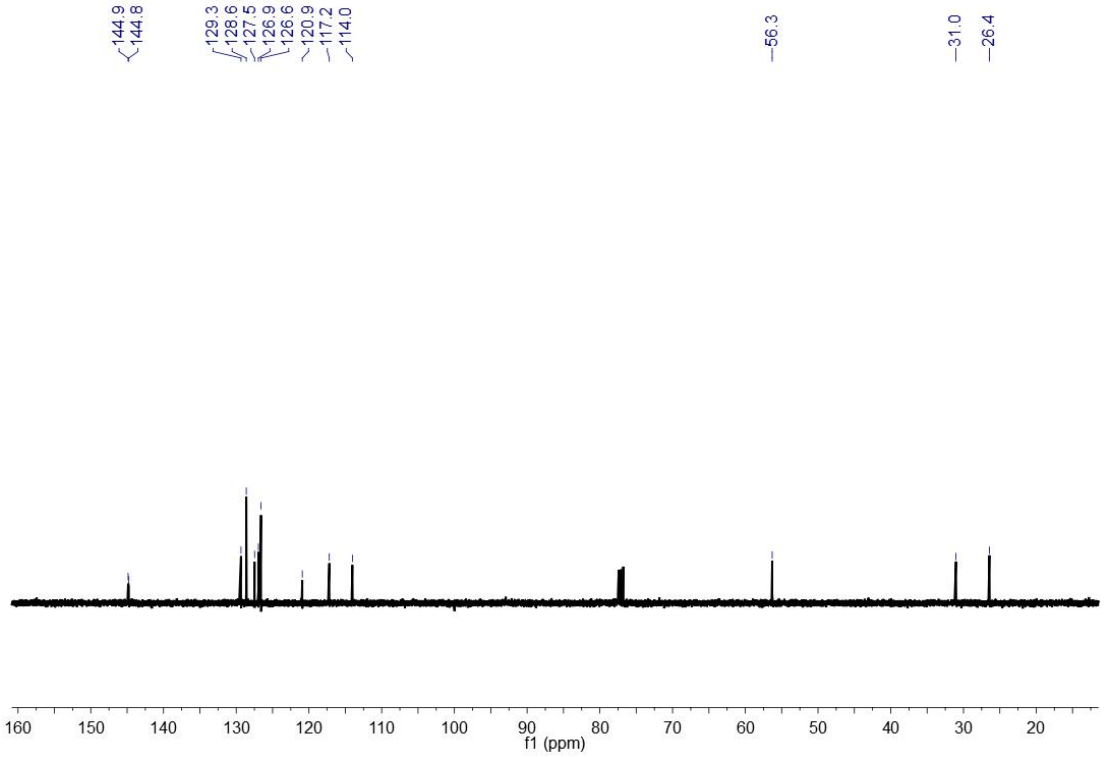
144.9
144.8
129.3
128.6
127.5
126.9
126.6
120.9
117.2
114.0
56.3
31.0
26.4
160 150 140 130 120 110 100 90 80 70 60 50 40 30 20
f1 (ppm)

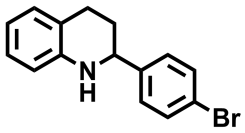
N
H
Br

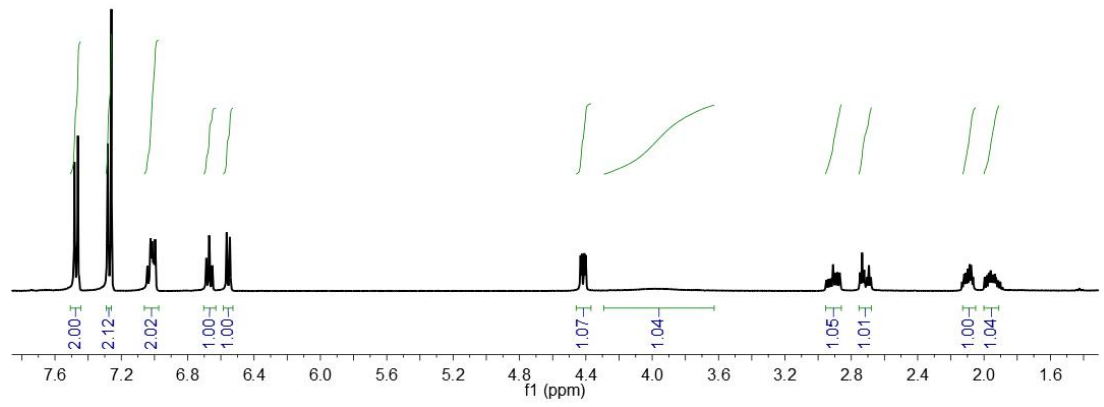
2.00
2.12
2.02
1.00
1.00
1.07
1.04
1.05
1.01
1.00
1.04
7.6 7.2 6.8 6.4 6.0 5.6 5.2 4.8 4.4 4.0 3.6 3.2 2.8 2.4 2.0 1.6
f1 (ppm)

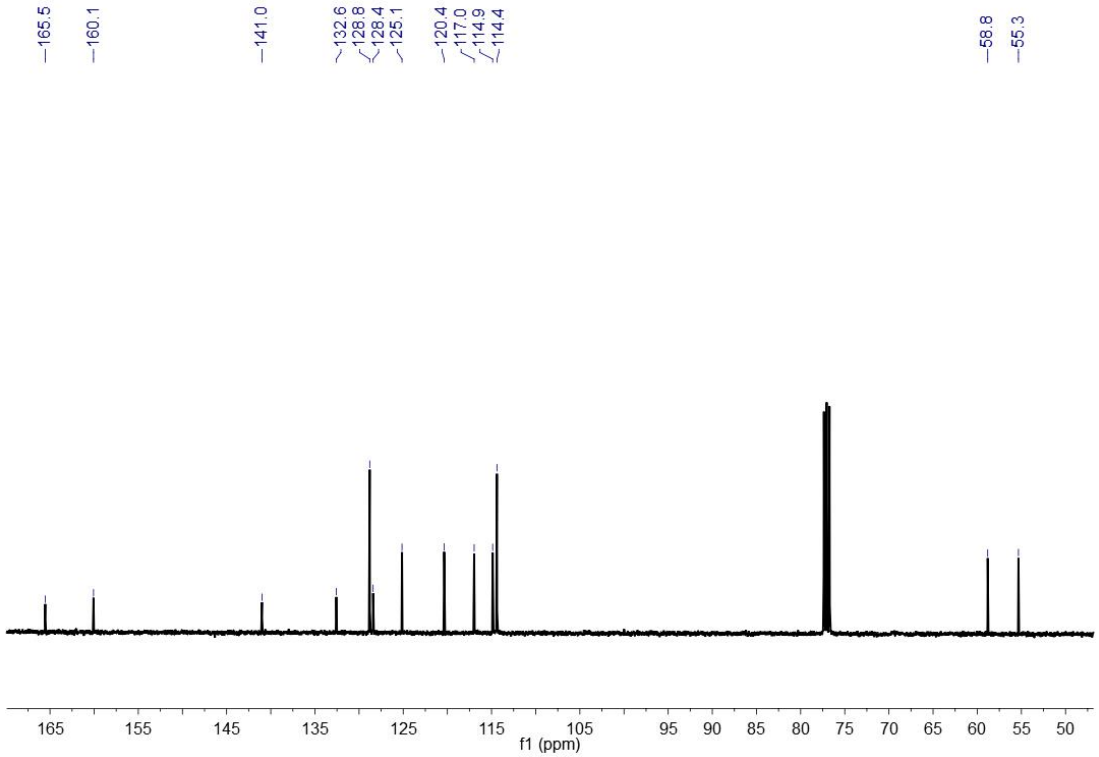
165.5
160.1
141.0
132.6
128.8
128.4
125.1
120.4
117.0
114.9
114.4
58.8
55.3
165
155
145
135
125
115
105
95
90
85
80
75
70
65
60
55
50
f1 (ppm)

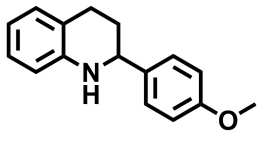
N
H
O

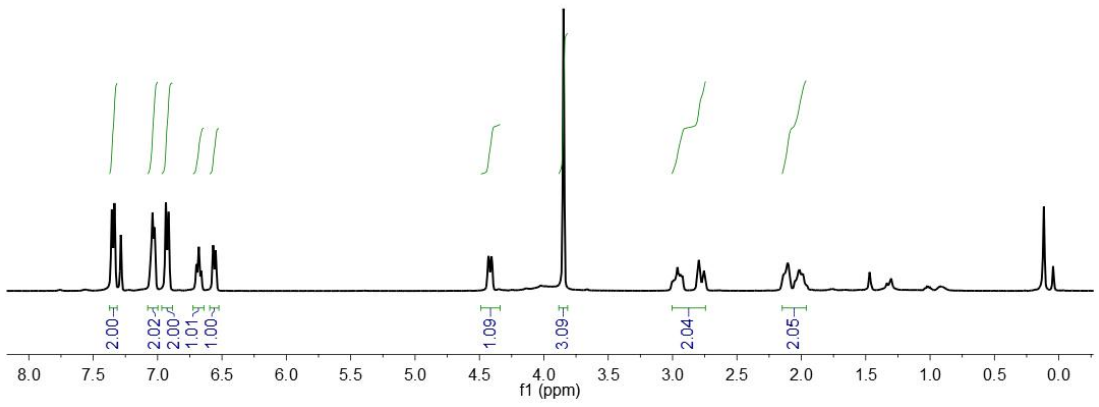
2.00
2.02
2.00
1.01
1.00
1.09
3.09
2.04
2.05
8.0
7.5
7.0
6.5
6.0
5.5
5.0
4.5
4.0
3.5
3.0
2.5
2.0
1.5
1.0
0.5
0.0
f1 (ppm)

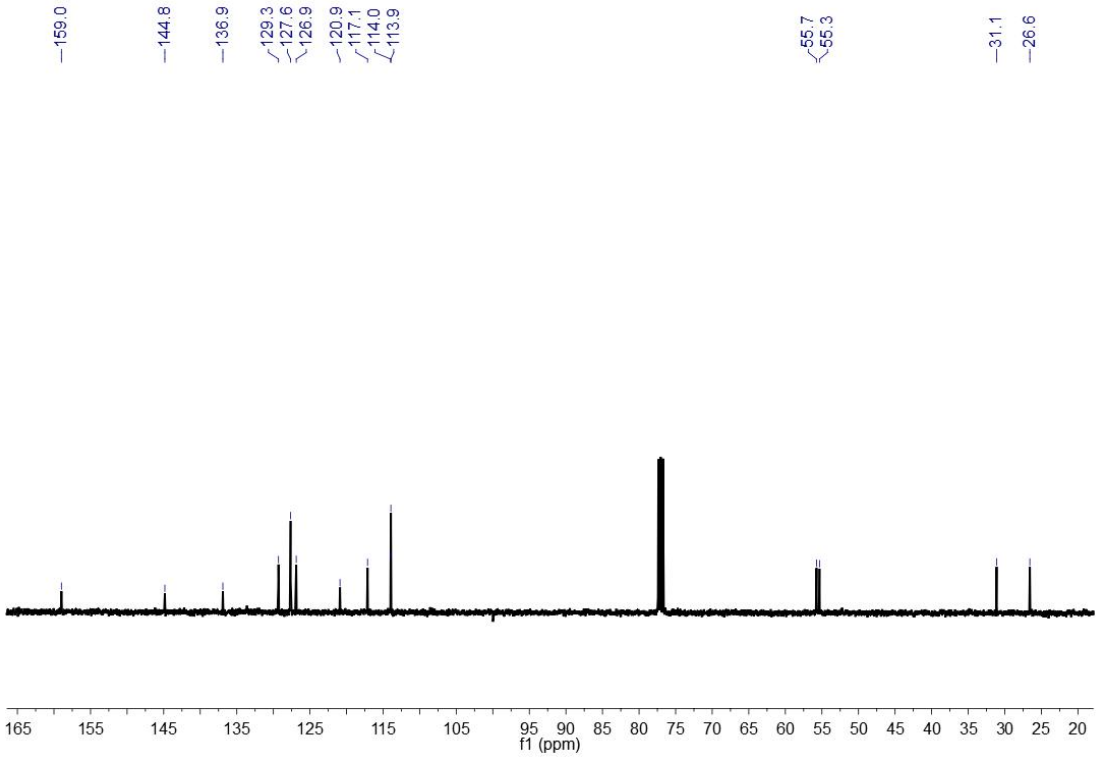
159.0
144.8
136.9
129.3
127.6
126.9
120.9
117.1
114.0
113.9
55.7
55.3
31.1
26.6
165 155 145 135 125 115 105 95 90 85 80 75 70 65 60 55 50 45 40 35 30 25 20
f1 (ppm)

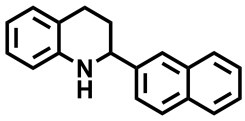
N
H

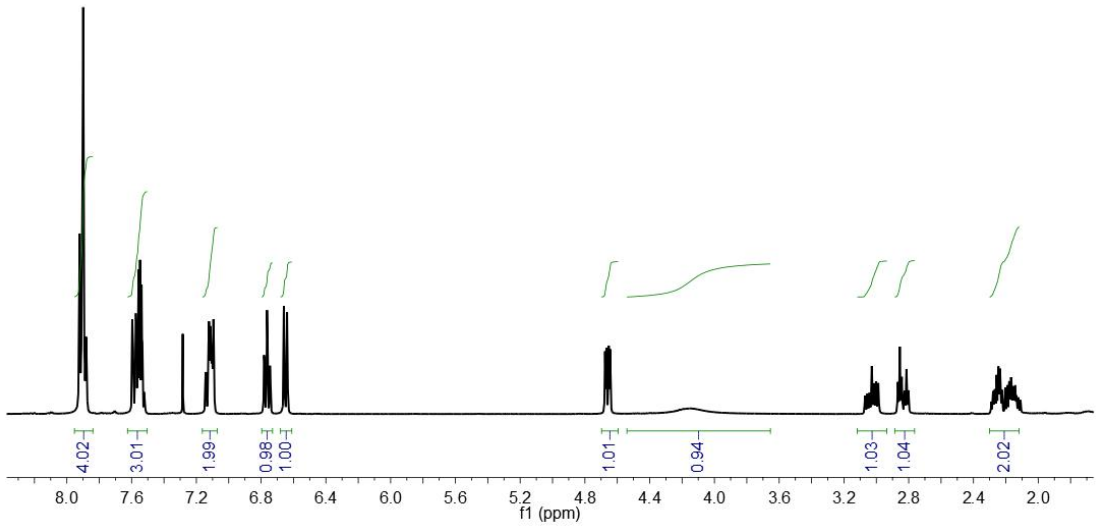
4.02
3.01
1.99
0.98
1.00
1.01
0.94
1.03
1.04
2.02
8.0 7.6 7.2 6.8 6.4 6.0 5.6 5.2 4.8 4.4 4.0 3.6 3.2 2.8 2.4 2.0
f1 (ppm)

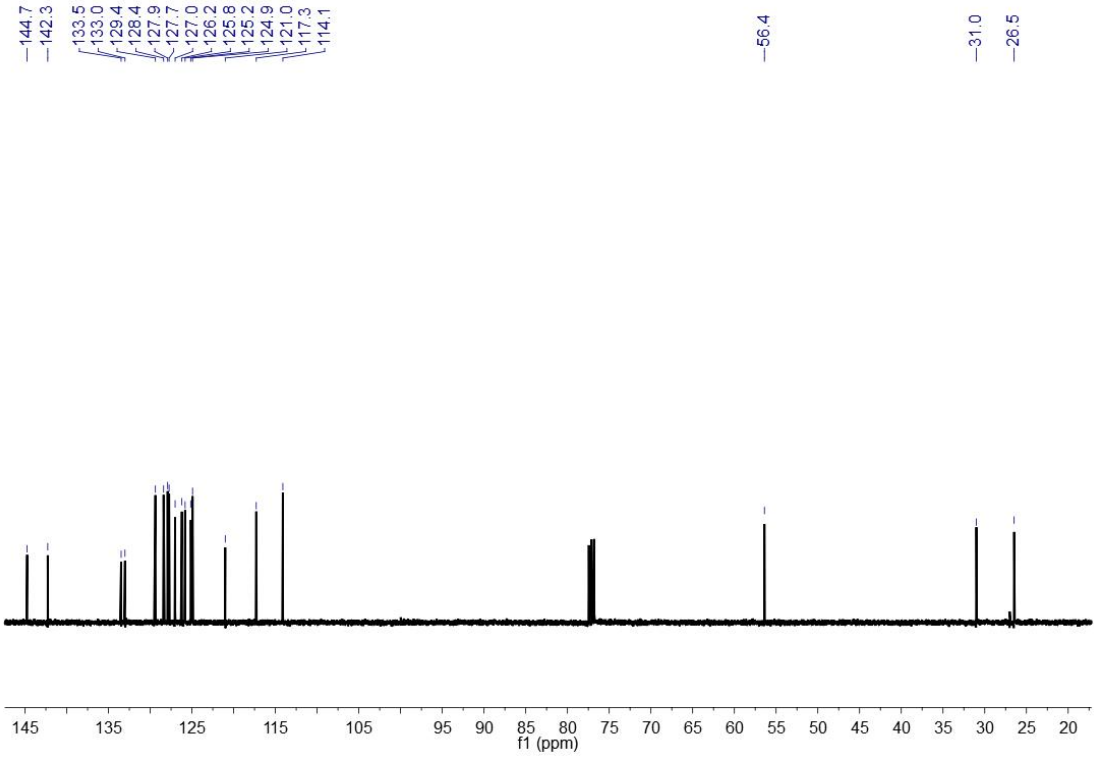
144.7
142.3
133.5
133.0
129.4
128.4
127.9
127.7
127.0
126.2
125.8
125.2
124.9
121.0
117.3
114.1
56.4
31.0
26.5
145 135 125 115 105 95 90 85 80 75 70 65 60 55 50 45 40 35 30 25 20
f1 (ppm)

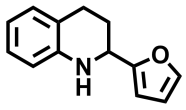
N
H
O

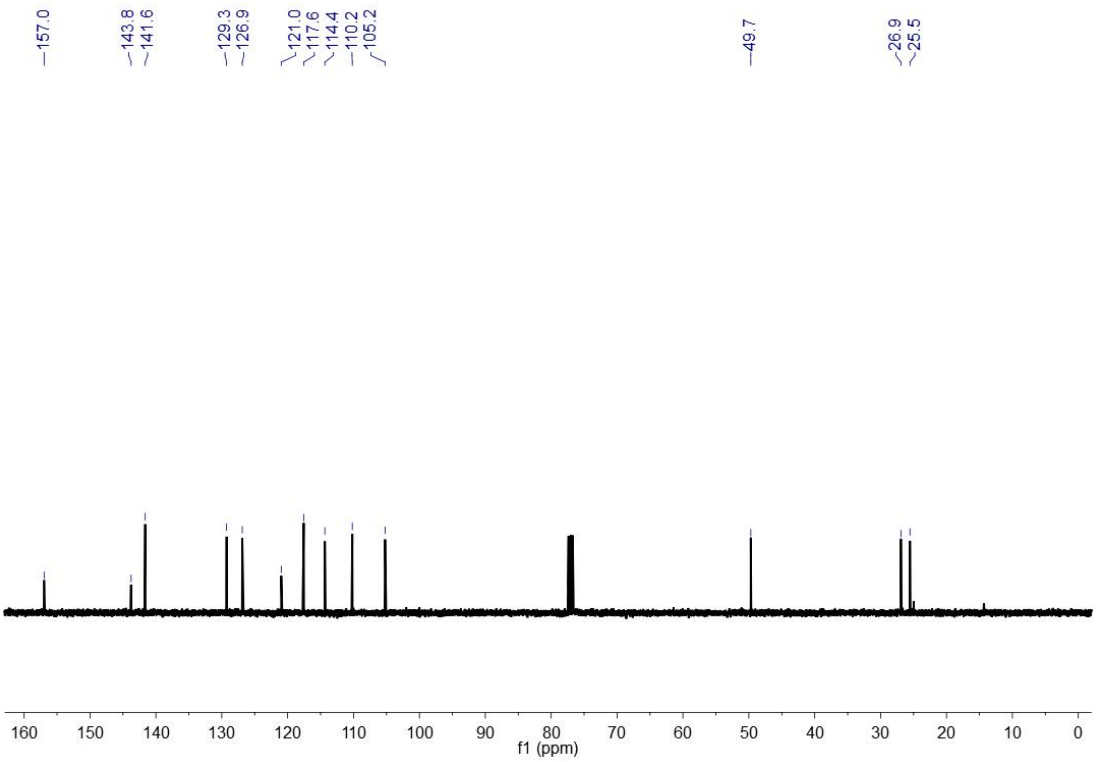
157.0
143.8
141.6
129.3
126.9
121.0
117.6
114.4
110.2
105.2
49.7
26.9
25.5
160 150 140 130 120 110 100 90 80 70 60 50 40 30 20 10 0
f1 (ppm)

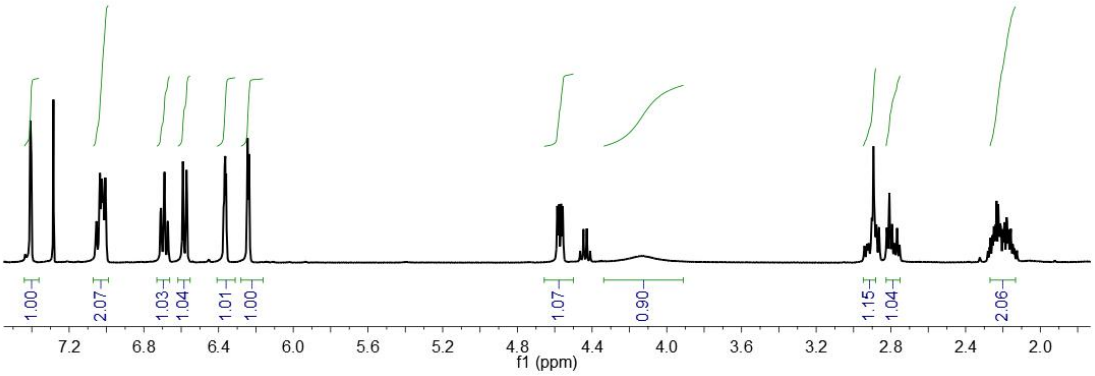
1.00
2.07
1.03
1.04
1.01
1.00
1.07
0.90
1.15
1.04
2.06
7.2
6.8
6.4
6.0
5.6
5.2
4.8
4.4
4.0
3.6
3.2
2.8
2.4
2.0
f1 (ppm)

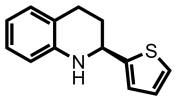
N
H
S

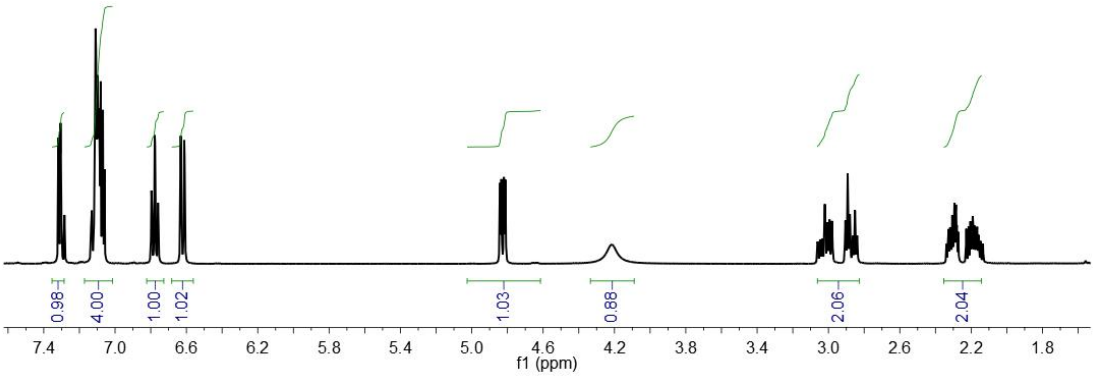
0.98
4.00
1.00
1.02
1.03
0.88
2.06
2.04
7.4
7.0
6.6
6.2
5.8
5.4
5.0
4.6
4.2
3.8
3.4
3.0
2.6
2.2
1.8
f1 (ppm)

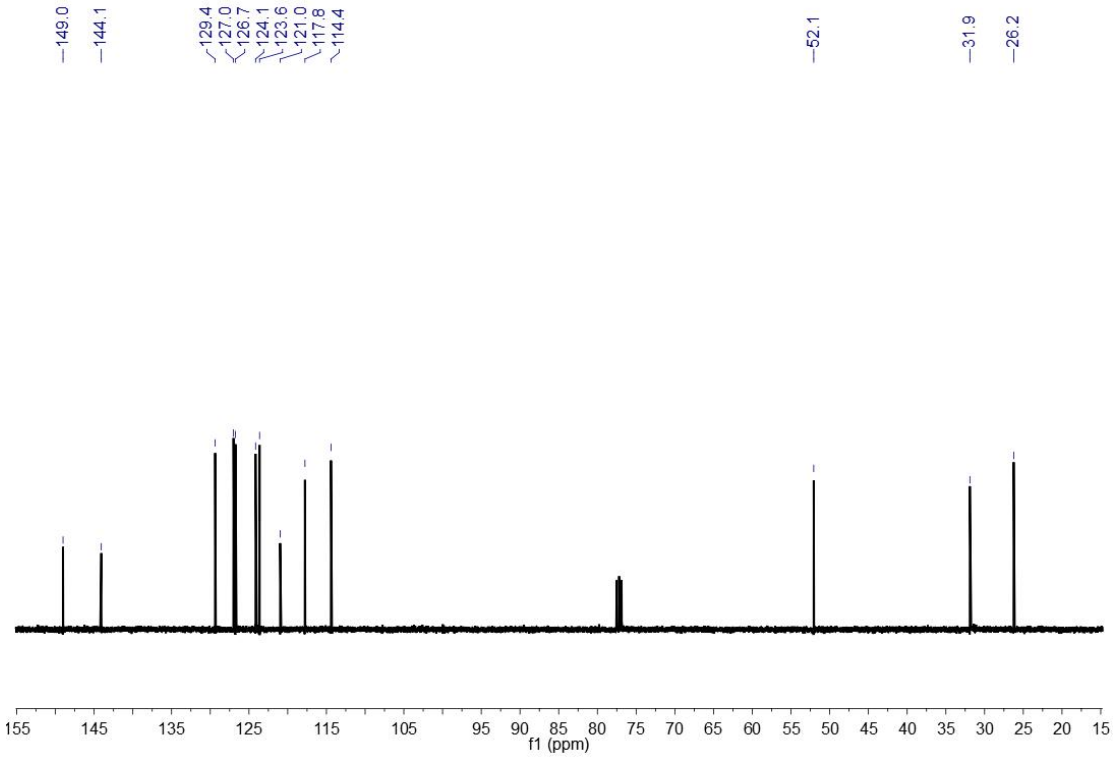

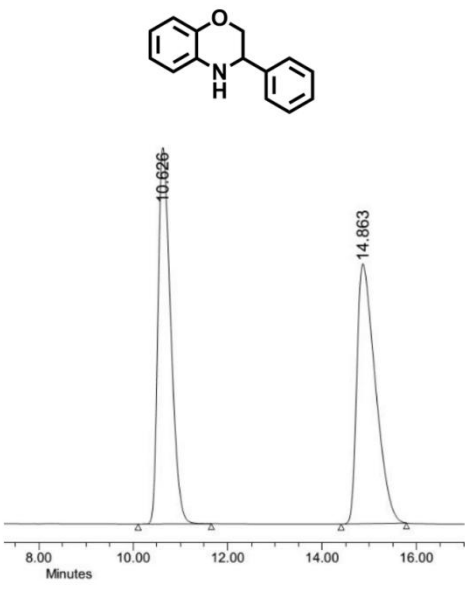

	RT (min)	Area (μV*sec)	% Area	Height (μV)	% Height
1	10.626	33941893	49.68	1834413	59.20
2	14.863	34374538	50.32	1264380	40.80

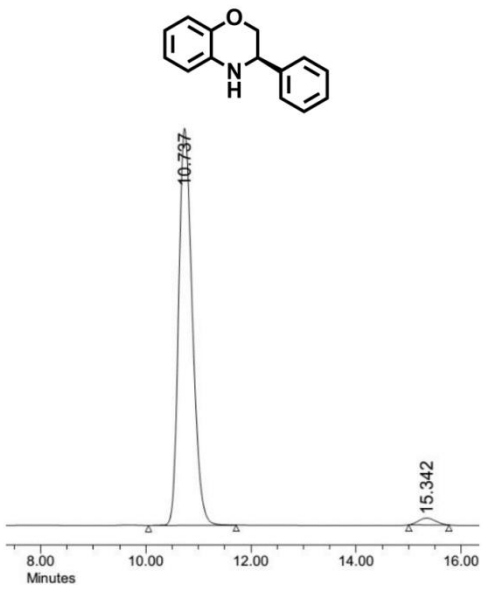

	RT (min)	Area (μV*sec)	% Area	Height (μV)	% Height
1	10.737	12741719	97.92	707127	98.31
2	15.342	270456	2.08	12136	1.69

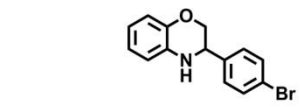

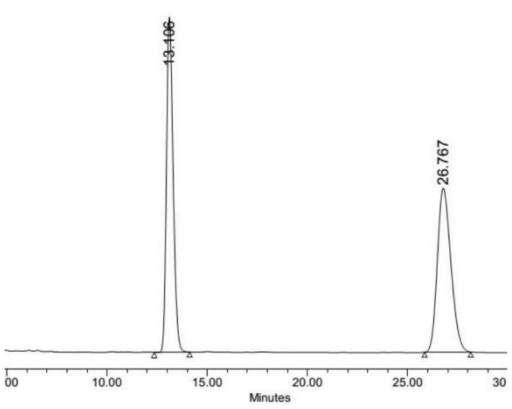

	RT (min)	Area (μV*sec)	% Area	Height (μV)	% Height
1	13.106	3543066	50.10	153919	67.16
2	26.767	3529522	49.90	75274	32.84

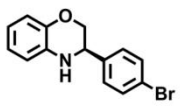

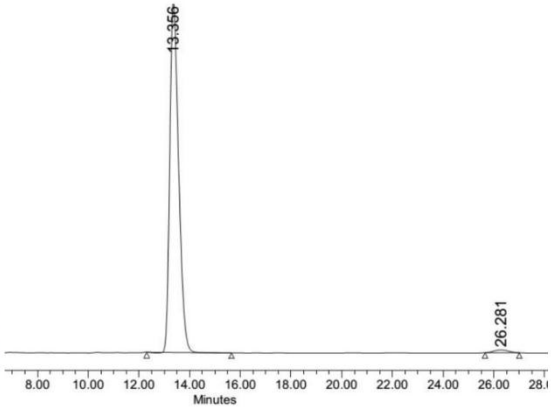

	RT (min)	Area (μV*sec)	% Area	Height (μV)	% Height
1	13.356	7038392	98.64	289827	99.18
2	26.281	96987	1.36	2406	0.82

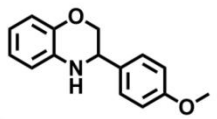

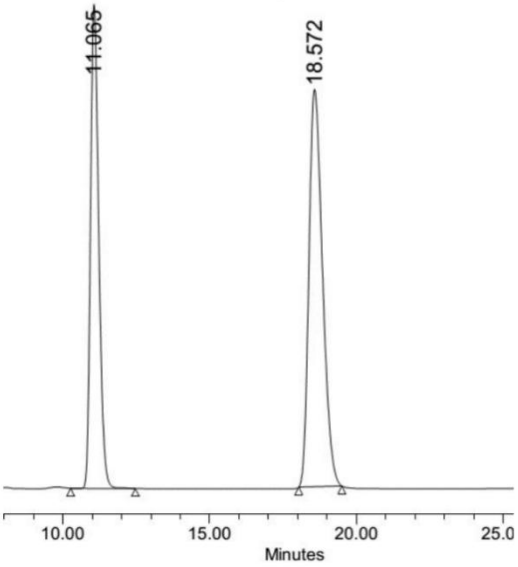

	RT (min)	Area (μV*sec)	% Area	Height (μV)	% Height
1	11.065	10076847	42.53	517952	54.91
2	18.572	13618247	57.47	425308	45.09

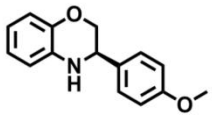

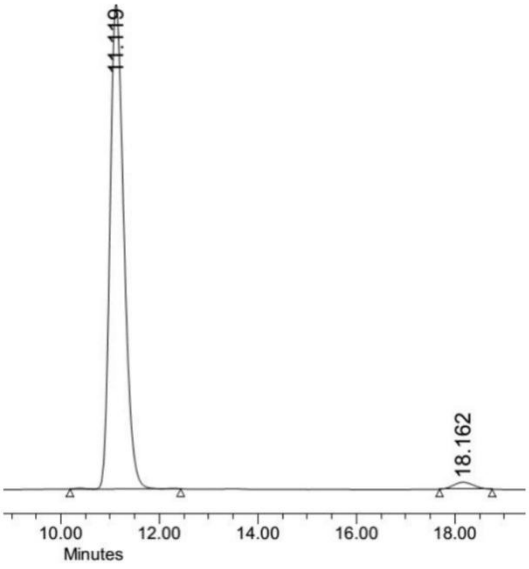

	RT (min)	Area (μV*sec)	% Area	Height (μV)	% Height
1	11.119	9352254	97.93	478898	98.58
2	18.162	197697	2.07	6903	1.42

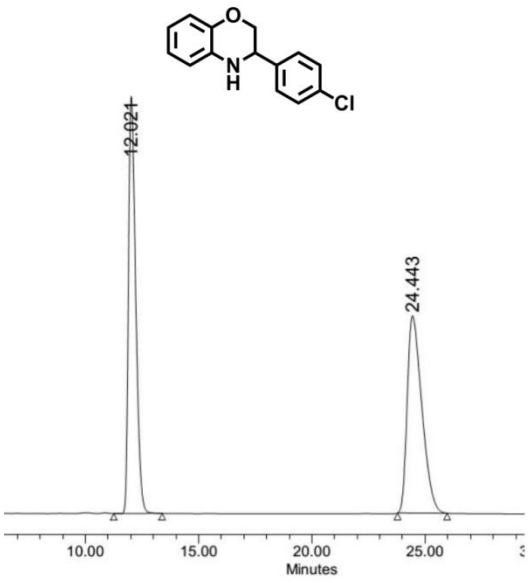

	RT (min)	Area (μV*sec)	% Area	Height (μV)	% Height
1	12.021	11795857	50.93	535632	67.93
2	24.443	11365976	49.07	252896	32.07

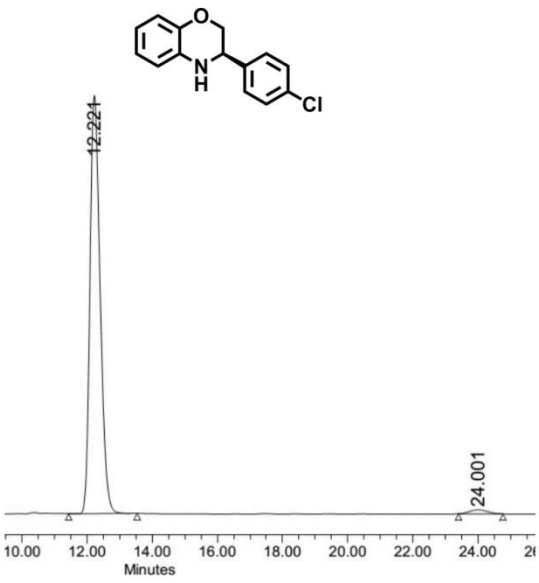

	RT (min)	Area (μV*sec)	% Area	Height (μV)	% Height
1	12.221	4665739	98.32	216383	99.05
2	24.001	79610	1.68	2078	0.95

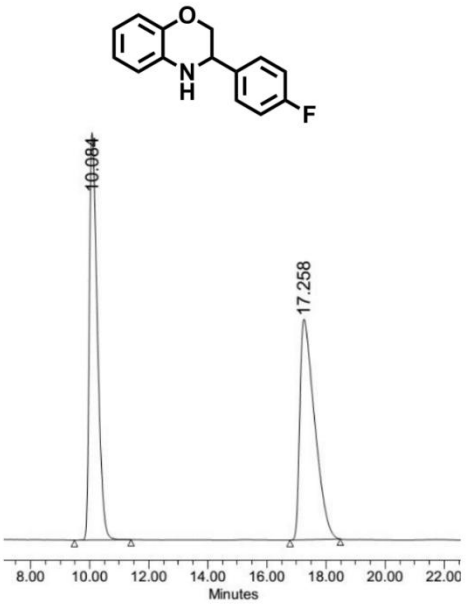

	RT (min)	Area (μV*sec)	% Area	Height (μV)	% Height
1	10.084	34056030	49.87	1817642	64.88
2	17.258	34227668	50.13	983908	35.12

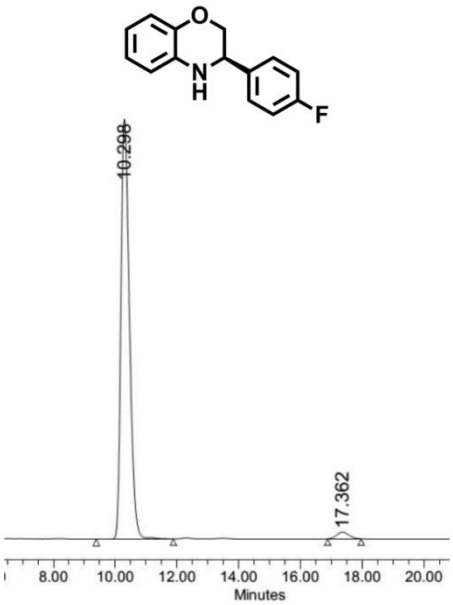

	RT (min)	Area (μV*sec)	% Area	Height (μV)	% Height
1	10.298	14496013	97.69	766323	98.40
2	17.362	343084	2.31	12426	1.60

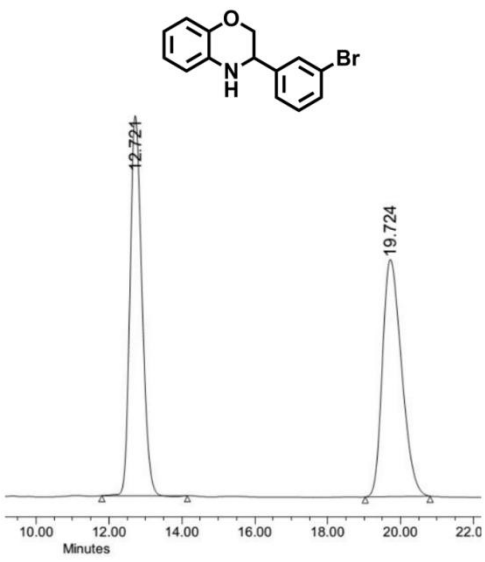

	RT (min)	Area (μV*sec)	% Area	Height (μV)	% Height
1	12.721	9797853	50.19	427971	61.59
2	19.724	9724947	49.81	266848	38.41

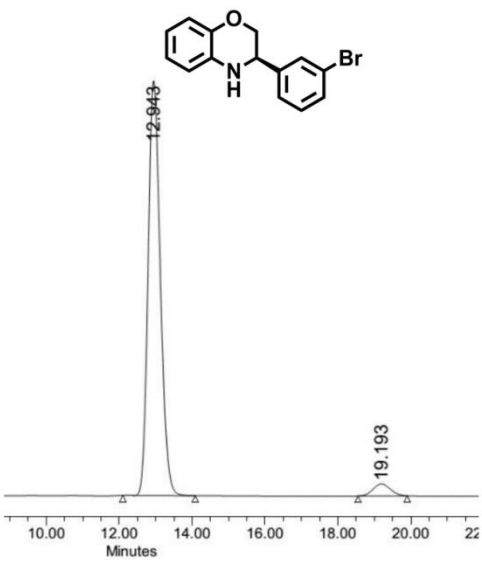

	RT (min)	Area (μV*sec)	% Area	Height (μV)	% Height
1	12.943	6046645	96.04	261259	97.19
2	19.193	249374	3.96	7542	2.81

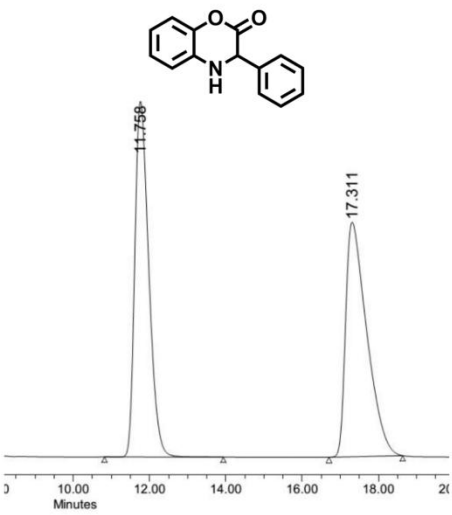

	RT (min)	Area (μV*sec)	% Area	Height (μV)	% Height
1	11.758	19931995	50.07	785391	60.30
2	17.311	19877903	49.93	517178	39.70

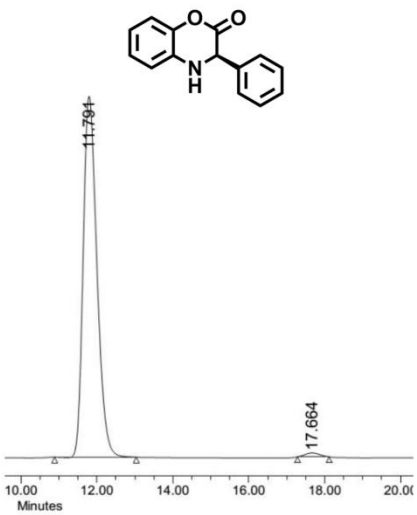

	RT (min)	Area (μV*sec)	% Area	Height (μV)	% Height
1	11.791	10386718	98.82	415833	98.92
2	17.664	123582	1.18	4529	1.08

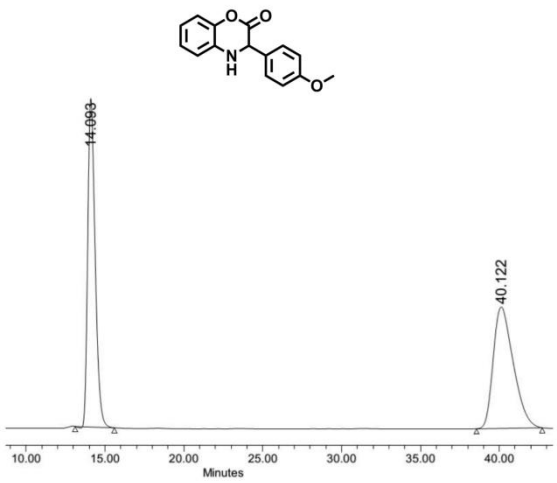

	RT (min)	Area (μV*sec)	% Area	Height (μV)	% Height
1	14.093	6226716	49.98	190428	73.01
2	40.122	6230798	50.02	70399	26.99

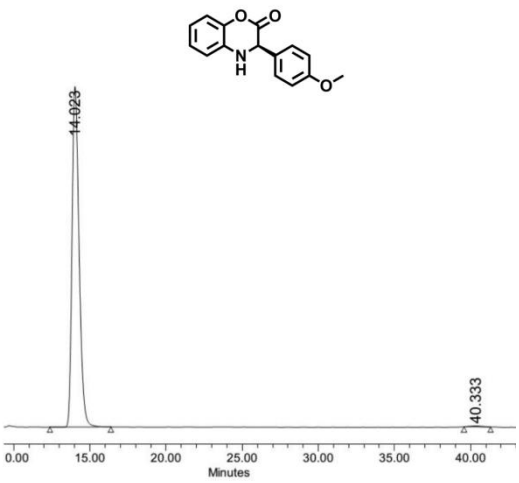

	RT (min)	Area (μV*sec)	% Area	Height (μV)	% Height
1	14.023	5974408	99.51	185891	99.74
2	40.333	29341	0.49	478	0.26

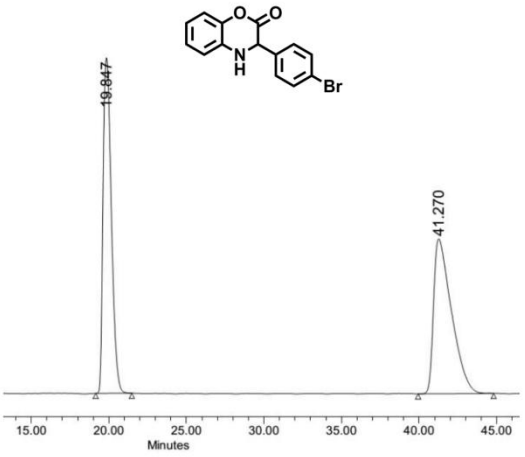

	RT (min)	Area (μV*sec)	% Area	Height (μV)	% Height
1	19.847	15745972	50.01	425349	68.41
2	41.270	15736949	49.99	196388	31.59

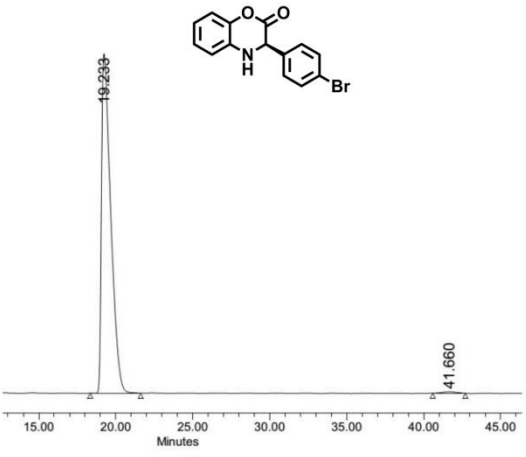

	RT (min)	Area (μV*sec)	% Area	Height (μV)	% Height
1	19.233	23538576	99.40	566525	99.59
2	41.660	142899	0.60	2359	0.41

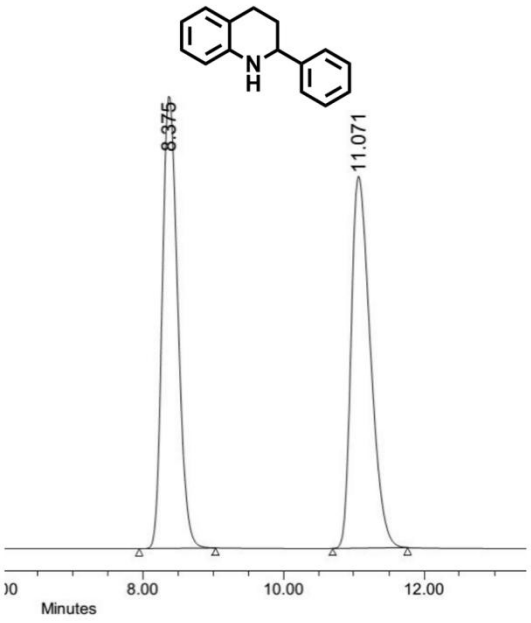

	RT (min)	Area (μV*sec)	% Area	Height (μV)	% Height
1	8.375	35145568	49.39	2307541	54.89
2	11.071	36009866	50.61	1896410	45.11

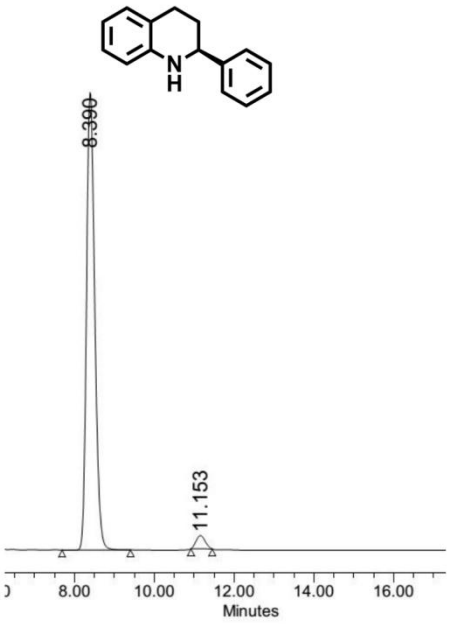

	RT (min)	Area (μV*sec)	% Area	Height (μV)	% Height
1	8.390	30547073	96.89	2144164	97.19
2	11.153	980717	3.11	62093	2.81

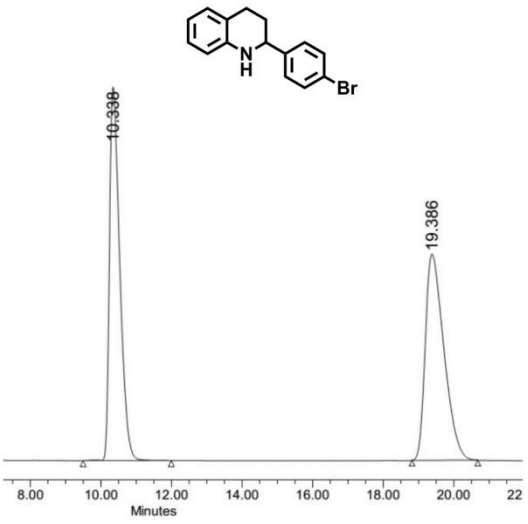

	RT (min)	Area (μV*sec)	% Area	Height (μV)	% Height
1	10.338	26912692	50.00	1328650	64.43
2	19.386	26911164	50.00	733380	35.57

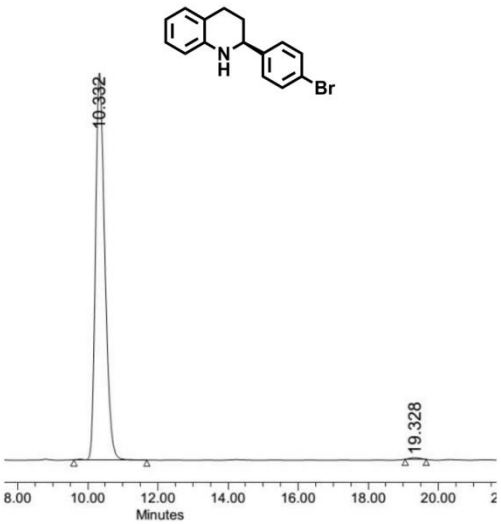

	RT (min)	Area (μV*sec)	% Area	Height (μV)	% Height
1	10.332	7143507	99.54	387555	99.61
2	19.328	32928	0.46	1536	0.39

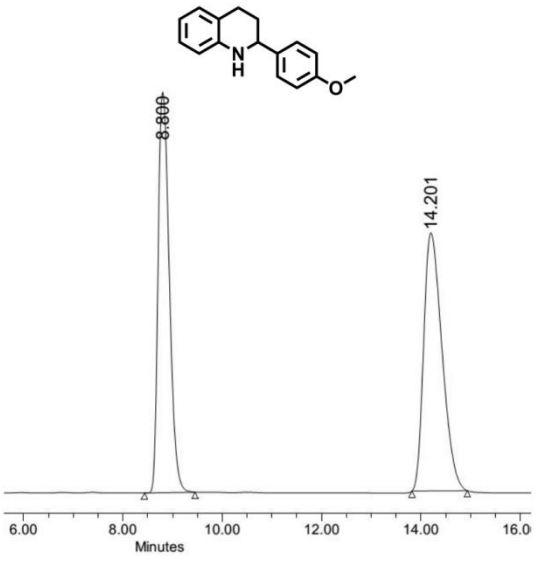

	RT (min)	Area (μV*sec)	% Area	Height (μV)	% Height
1	8.800	38991068	48.46	2506645	60.82
2	14.201	41468528	51.54	1614756	39.18

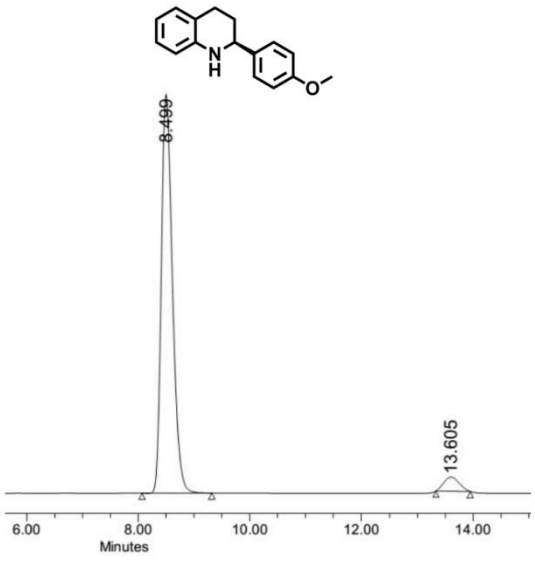

	RT (min)	Area (μV*sec)	% Area	Height (μV)	% Height
1	8.499	25997598	95.31	1880483	96.58
2	13.605	1279705	4.69	66492	3.42

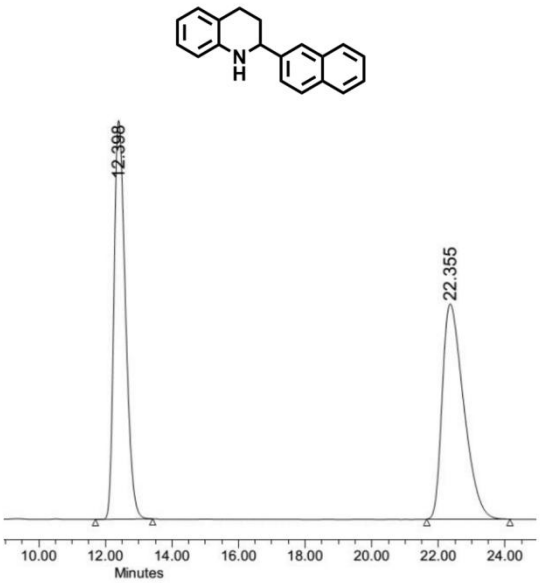

	RT (min)	Area (μV*sec)	% Area	Height (μV)	% Height
1	12.398	49943444	49.69	2092495	64.94
2	22.355	50572289	50.31	1129787	35.06

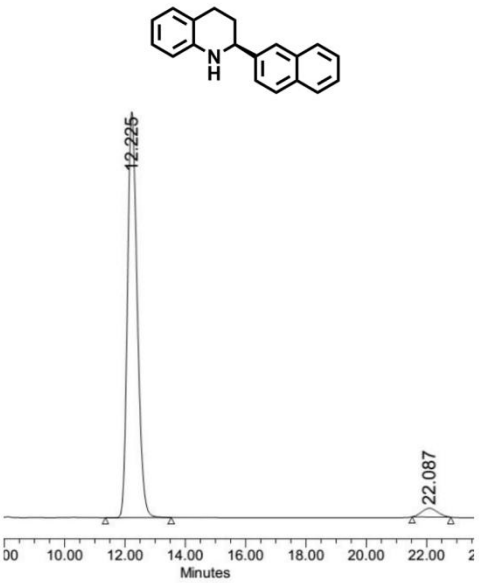

	RT (min)	Area (μV*sec)	% Area	Height (μV)	% Height
1	12.225	21234099	96.59	944848	97.89
2	22.087	748904	3.41	20358	2.11

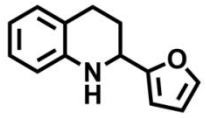

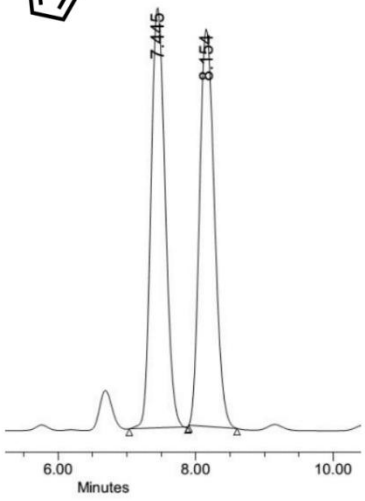

	RT (min)	Area (μV*sec)	% Area	Height (μV)	% Height
1	7.445	30681817	50.36	2137549	51.41
2	8.154	30241138	49.64	2020464	48.59

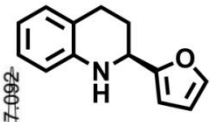

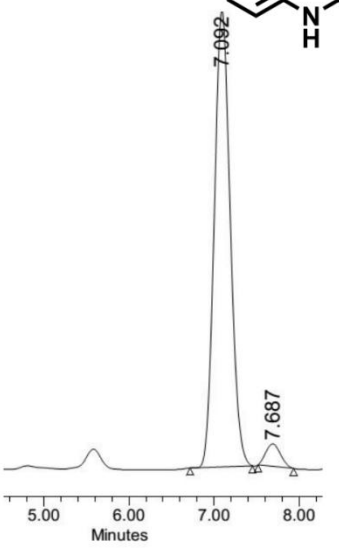

	RT (min)	Area (μV*sec)	% Area	Height (μV)	% Height
1	7.092	6465286	95.68	497879	95.32
2	7.687	291732	4.32	24430	4.68

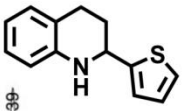

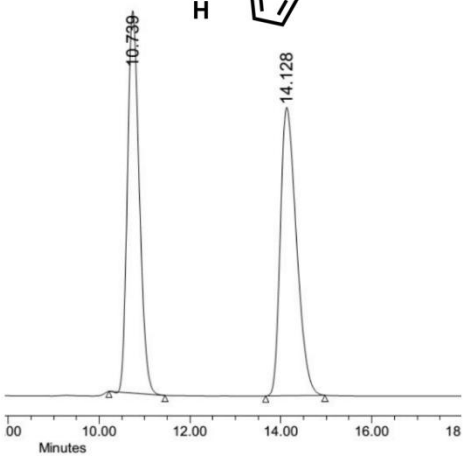

	RT (min)	Area (μV*sec)	% Area	Height (μV)	% Height
1	10.739	28608733	49.27	1582992	57.02
2	14.128	29454967	50.73	1193390	42.98

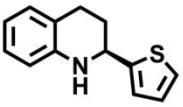

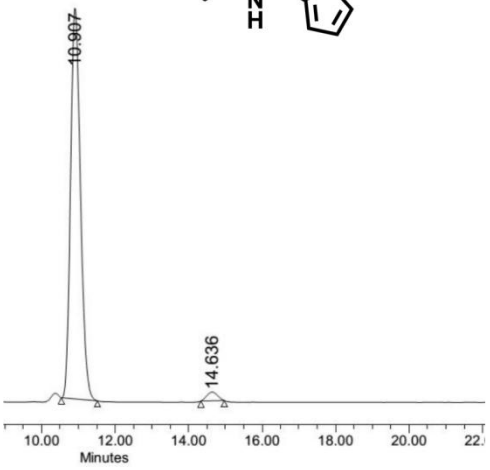

	RT (min)	Area (μV*sec)	% Area	Height (μV)	% Height
1	10.907	13826073	97.63	743389	97.82
2	14.636	336167	2.37	16536	2.18

Section 7. References

1. T. R. Wu, L. Shen, J. M. Chong, *Org. Lett.,* 2004, **6**, 2701−2704.

2. C. Michon, F. Medina, M. Abadie, F. Agbossou-Niedercorn, *Organometallics,* 2013*,* **32***,* 5589−5600*.*

3. (*a*) M. Yamanaka, J. Itoh, K. Fuchibe, T. Akiyama, *J. Am. Chem. Soc.,* 2007, **129**, 6756–6764; (*b*) F. Romanov-Michailidis, M. Romanova-Michaelides, M. Pupier, A. Alexakis, *Chem. Eur. J.,* 2015, **21**, 5561–5583.

4. W. Hu, J. Zhou, X. Xu, W. Liu, L. Gong, *Org. Synth.,* 2011, **88**, 406−417.

5. (*a*) C. Bleschke, J. Schmidt, D. S. Kundu, S. Blechert and A. Thomas, *Adv. Synth. Catal.,* 2011, **353**, 3101-3106; (*b*) D. S. Kundu, J. Schmidt, C. Bleschke, A. Thomas and S. Blechert, *Angew. Chem. Int. Ed.*, 2012, **51**, 5456-5459; (*c*) X. Zhang, A. Kormos and J. Zhang, *Org. Lett.*, 2017, **19**, 6072-6075; (*d*) J. Wang, Z. H. Zhu, M. W. Chen, Q. A. Chen and Y. G. Zhou, *Angew. Chem. Int. Ed.,* 2019, **58**, 1813-1817; (*e*) J. Wang, Z. B. Zhao, Y. Zhao, G. Luo, Z. H. Zhu, Y. Luo and Y. G. Zhou, *J. Org. Chem.*, 2020, **85**, 2355-2368; (*f*) Z. P. Chen, M. W. Chen, R. N. Guo and Y. G. Zhou, *Org. Lett.*, 2014, **16**, 1406-1409; (*g*) X. Li, J. J. Tian, N. Liu, X. S. Tu, N. N. Zeng and X. C. Wang, *Angew. Chem. Int. Ed.*, 2019, **58**, 4664-4668; (*h*) X. F. Cai, W. X. Huang, Z. P. Chen and Y. G. Zhou, *Chem. Commun.*, 2014, **50**, 9588-9590; (*i*) J. Wen, R. Tan, S. Liu, Q. Zhao and X. Zhang, *Chem. Sci.*, 2016, **7**, 3047-3051; (*j*) S. Sun and P. Nagorny, *Chem. Commun.*, 2020, **56**, 8432-8435; (*k*) K. Gao, C.-B. Yu, D.-S. Wang and Y.-G. Zhou, *Adv. Synth. Catal.*, 2012, **354**, 483-488; (*l*) H. J. Pan and X. Hu, *Angew. Chem. Int. Ed.*, 2020, **59**, 4942-4946; (*m*) Y. Liu, F. Chen, Y. M. He, C. Li and Q. H. Fan, *Org. Biomol. Chem.*, 2019, **17**, 5099-5105; (*n*) J. Qin, F. Chen, Y.-M. He and Q.-H. Fan, *Org. Chem. Front.*, 2014, **1**, 952-955; (*o*) X. C. Zhang, Y. H. Hu, C. F. Chen, Q. Fang, L. Y. Yang, Y. B. Lu, L. J. Xie, J. Wu, S. Li and W. Fang, *Chem. Sci.*, 2016, **7**, 4594-4599.